A NOVEL BIOMECHANICAL MODEL ASSESSING ORTHODONTIC, CONTINUOUS ARCHWIRE ACTIVATION IN INCOGNITO LINGUAL BRACES

Christopher Howard Canales, DMD

A thesis submitted to the faculty of the University of North Carolina at Chapel Hill in partial fulfillment of the requirements for the degree of Master of Science in the School of Dentistry (Orthodontics).

Chapel Hill
2011

Approved by

Advisor: Ching-Chang Ko

Reader: Rose Sheats

Reader: Clarke Stevens

ABSTRACT

CHRISTOPHER HOWARD CANALES:

A Novel Biomechanical Model Assessing Orthodontic, Continuous Archwire Activation in Incognito Lingual Braces

(Under the direction of Dr. Ching-Chang Ko)

The purpose of this research is to develop a virtual, orthodontic, continuous archwire model for assessing a lingual bracket system. A digital model of a maxilla, periodontal ligament, and dentition was constructed from human computed tomography data. Virtual lingual and facial brackets were placed on the maxillary left central incisor through first premolar. An intrusive tooth movement was utilized to test the model and compare labial and lingual biomechanics. The ANSYS 13.0 birth-death function simulated force interaction between the wire and brackets.

The goal of placing labial and lingual bracket-wire systems on accurate anatomy including multiple teeth was achieved. Material property definitions had an effect on a finite element model. The birth-death computer technique simulated the clinical effects of placing an archwire in brackets and allowing forces to be transferred from the bracket-wire system to the surrounding dental structures. The lingual appliance has different biomechanical effects than the labial appliance.

ACKNOWLEDGEMENTS

I would like to thank the following for their contribution, support and dedication:

Dr. Ching-Chang Ko, for his mentorship, support and encouragement throughout this project. He helped make the most of this life-death situation (or birth-death).

Dr. Rose Sheats, for her help and advice in completing the manuscript.

Dr. Clarke Stevens, for providing the virtual facial brackets used in this research and his input on the final manuscript.

Dr. Dirk Wiechmann, for providing the virtual Incognito brackets used in this study.

Dr. Matt Larson, for his assistance with the ANSYS software. His contribution was above and beyond the call of duty.

Dr. Dan Grauer, for your time and assistance with analysis and manuscript.

Dr. Angie Halverson, for her love, support, and patience.

My family for always providing me with their love and encouragement.

TABLE OF CONTENTS

LIST OF TABLES

LIST OF FIGURES

I INTRODUCTION

Current options for invisible orthodontic appliances include clear brackets, clear aligners, and lingual braces. The use of clear brackets has grown due to the esthetic improvement over conventional metal brackets (1). Invisalign, the most popular clear aligner system, has recently surpassed one million started cases even though clear aligner trays have significant biomechanical limitations and require additional training (2). The trend toward esthetic appliances is pronounced. Most recently, a low-profile lingual bracket named Incognito has been developed to combine esthetics and patient comfort while maintaining traditional biomechanical advantages of fixed appliances (3-6).

Clinical research assessing Incognito has demonstrated reasonable patient and doctor acceptability (7, 8). The number of lingual cases started is, however, low compared to labial systems. Part of this is due to unfamiliar biomechanics inherent in the lingual system. The purpose of this research is to develop a new orthodontic, continuous archwire model for assessing lingual biomechanics. A simple and clinically realistic intrusive tooth movement was utilized to test the model and compare the biomechanics between the lingual and the labial systems.

In the following text, the clinical aspects of Incognito, the current knowledge of lingual biomechanics, and current biomechanical studies in orthodontics will be reviewed.

II BACKGROUND

Incognito Lingual System

The development of custom, low-profile lingual brackets (Incognito) has addressed several problems experienced by the patients and clinicians who used conventional lingual brackets. These include patient comfort, rebonding debonded brackets, and making finishing archwire bends. Studies of conventional lingual appliance systems have examined patient motivation and comfort levels, hygienic properties, and effect on speech (3-5). Miyawaki et al (9) surveyed 111 post-treatment patients who were treated with combinations of labial and conventional lingual brackets (Kurz appliance 7th generation, Ormco) for upper and lower dental arches. For those treated with lingual appliances, 57% to 76% of patients reported problems with chewing, tongue soreness, difficulty in tooth brushing, and problems pronouncing s and t sounds. All these factors were significantly higher than those treated with labial appliance. 20% to 46% of patients felt discomfort until after the removal of the lingual appliances.

A clinical trial has shown that patients were substantially more comfortable, and reported fewer problems and shorter adaptation times with Incognito appliances over conventional lingual appliances (3). Fritz et al (7) surveyed 98 patients about their experience with the Incognito system. 79% reported seeking orthodontic treatment for esthetic concerns and 53% would have refused treatment with ceramic labial brackets. Fritz also found that the most common type of patient who would choose lingual brackets were females below 40 years of age, who had a particular preference for esthetic treatment. 65% of patients reported injury or irritation and restricted functional space for the tongue. Speech disturbances including lisping were reported by 24% of patients. The phonetic-functional

adaptation period was determined by 82% of those surveyed to be 1–3 weeks. This differed from past surveys of patients treated with conventional lingual bracket systems, where about one third needed longer than three weeks to adapt to the appliances. 99% of the patients were happy with the outcome of their treatment. 87% would recommend the lingual appliance system to others without reserve.

Van der Veen et al (10) examined the difference in caries rate between buccal and lingual appliances. A split-mouth design assigned subjects to receive either buccal or lingual brackets on the upper arch and the alternative bracket type in the lower. The results indicated that buccal surfaces developed white spot lesions more frequently especially when some lesions existed before treatment. The number of white spot lesions found on buccal surfaces was 4.8 times higher than the number on lingual surfaces. Using quantitative light-induced fluorescence (QLF), the increase in integrated fluorescence loss was 10.6 times higher on the buccal than lingual.

The customized Incognito brackets address clinicians' problems in terms of bracket de-bonding/rebonding, and making finishing archwire bends. The custom brackets were designed with three characteristics that facilitate rebonding. First, the custom bracket pad was extended to cover most of the lingual tooth surface with contours that match each individual tooth. Bracket base thickness was increased to decrease the likelihood of bending. Finally, custom bracket design is modified to prevent occlusion on the bracket occlusal margins at both the initial position of the teeth and at the ideal final tooth position. Custom prescription brackets and robot-formed archwires are based on a setup of the desired outcome minimize the need finishing bends (3).

Grauer et al examined 94 consecutively treated cases measuring the ability of the lingual system to reach predetermined treatment results in terms of a six-degrees-of-freedom coordinate system. Discrepancies between the pre-planned tooth position and the final outcome were generally less than 1 mm and 4 degrees of rotation (except for 2nd molars) indicating that the fully customized lingual brackets are very accurate in achieving pre-planned treatment goals (11).

In summary, the Incognito system has proven to achieve patient acceptance and accurate clinical results. It seems logical that the next step would be to determine the biomechanics of the lingual appliance and highlight differences with conventional labial appliances.

Lingual Biomechanics

Understanding the biomechanics involved in lingual orthodontic systems will improve treatment efficiency and avoid possible side effects arising from forces exerted by the appliances. A comparison to familiar labial biomechanics will help fill the knowledge gap regarding forces and moments applied on the lingual side. The fundamental difference in the labial and lingual systems, from which all biomechanical differences stem, is the location where force is applied to the teeth. Geron et al (12) described a trigonometric function to highlight the theoretical differences (Figure 1). The distance between the bracket slot and the center of resistance is smaller with lingually-placed brackets, therefore the moment of a force is smaller. The effects of this relationship are most apparent when vertical forces are applied. The response to vertical forces is dependent on the initial tooth inclination and bracket position.

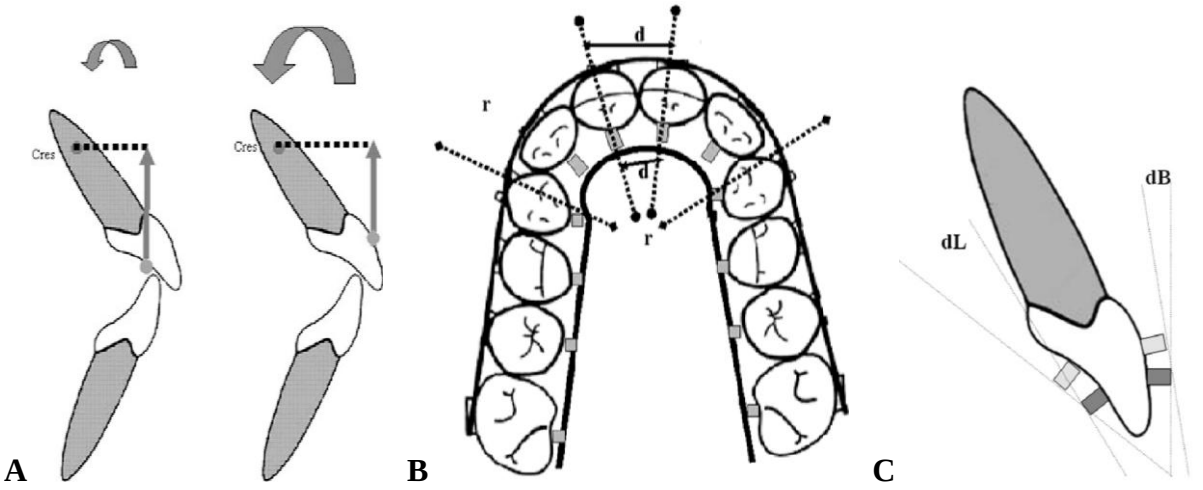

Figure 1. A, Slot position of labial versus lingual appliances relative to the center of resistance result in differing moments when equal forces are applied to each; **B,** Arch perimeter and inter-bracket distance is different for labial and lingual; **C,** Anatomic contours of the labial and lingual crown surfaces differ causing varying amounts of change when vertical bracket position changes. Illustrations are from Geron et al (12).

The perimeter of the dental arch is smaller on the lingual side than on the buccal making the inter-bracket distance smaller. Archwire load-deflection rate is much higher and activation range is reduced meaning that the effects of the equivalent archwires will be amplified on the lingual side, and therefore the accuracy of the lingual slot is crucial. Finally, the anatomy in labial and lingual tooth surfaces is different. Since the change in curvature of lingual surfaces is greater, equal displacement of a bracket in the occlusogingival direction will cause a more profound change in the slot torque. Geron stipulated that changes in placement along the mesiodistal surface of the tooth can cause more profound rotational effects with the lingual system due to greater differences in lingual anatomy.

Moran et al (13) conducted laboratory testing to determine the differences in inter-bracket distances and to quantify the effect on relative wire stiffness. 30 sets of post-

treatment models were measured to determine the mean inter-bracket distance for both "A" company labial brackets and Ormco lingual brackets. A ratio of lingual/labial anterior inter-bracket distance of 1:1.47 was found. 25 commonly used archwires were then evaluated for stiffness in bending and torsion as a function of overall anterior inter-bracket distance ratio. A cantilever tool measured the wires in first and second order while torque gauges measured third order. Results showed that the decreased inter-bracket distance with the lingual system can make a wire behave 3 times stiffer in the first and second order and 1.5 times stiffer in the third order than with facial appliances. This emphasizes the necessity of using lighter wires in the lingual system due to the decreased inter-bracket distance.

To examine the effect of labial versus lingual brackets, Fuck et al (6) conducted laboratory analysis using sensors to measure differences in both systems by placing brackets on identical casts of various malocclusions. Ten casts of patients undergoing orthodontic treatment were duplicated, sectioned between the teeth, and bonded with Incognito lingual brackets or 0.018-inch slot, Roth prescription, Diamond twin brackets. A 0.016-inch Sentalloy leveling archwire was placed. A sensor capable of measuring forces and moments was used to evaluate each tooth with the buccal wire engaged and then the lingual. By sequentially placing the sensor in place of each crown, the force applied from the complete system to each individual tooth was measured. As expected, results showed that the magnitude of most force and moment components were similar for both systems. Only first molars had significantly more force with the lingual system. Lingual appliances showed rotational moments that were significantly larger while tipping forces were significantly smaller. This was explained by the different configuration of the lingual bracket slot with vertical insertion of the wire in the anterior teeth.

The aforementioned studies were limited by their bench-top designs. None of these studies considered biological properties due to lack of tissues (bone, PD, and teeth) included in the models. The previous studies usually looked at only limited aspects of often complex biomechanical situations rather than the effects of the entire system. As a result, the conclusion of the lingual biomechanics is still uncertain, which require a new biomechanical tool for further clarification.

Computational Orthodontic Biomechanics

In vivo methods that directly measure internal stress without altering the tissues do not currently exist. The advances in computer modeling techniques provide another option to realistically estimate stress distribution (14-22). The finite element analysis (FEA), a computer simulation technique, utilizes the Ritz method of numerical analysis and minimization of variational calculus to obtain approximate solutions to mechanical stress and deformation of complex structures (19). The FEA has been widely used to predict the biomechanical performance of various medical devices and biological tissues. Unlike other methods which are limited to points on the surface, the finite element method can quantify stresses and displacement throughout the anatomy of a three dimensional structure (19). Since Farah's early work in restorative dentistry in 1973, the popularity of the FEA has grown (23). Early models were two dimensional and often limited by the high number of calculations necessary to provide useful analysis. As advancements have been made in computer and software capability, more complex structures have been simulated in greater detail.

To provide more accurate anatomic structures, Cattaneo has used images from a micro-CT scan with a voxel dimension of 37 micrometers and sequentially stacked 2-D slices

to form a 3-D model using Mimic software (17, 20, 21). With a goal of describing the overall behavior of the periodontal ligament (PDL), Cattaneo et al (17) constructed a model containing a segment of mandible and two teeth and applied point forces to simulate forces of a labial bracket system. The PDL was modeled as a bilinear, elastic material as opposed to linear elastic as in most previous finite element models. Material properties (Young's modulus and Poisson's ratio) assigned to bone were either homogeneous or varied based on the density of the bone. For the PDL, 3 different properties were examined. Two were linear with different Young's moduli and one was non-linear. The non-linear behavior reflected contact between roots and bone in compression as well as fiber disruption in tension. Two types of forces were applied: uncontrolled tipping with a point force and a force combined with a moment to represent translation. Results showed tension and compression areas with linear PDL material properties. For non-linear PDL properties, tension was more predominant than compression and much less load was applied in compression areas.

Cattaneo et al (21) aimed to demonstrate the influence of PDL material properties on the type of tooth movement while utilizing the same model as the 2005 study. The non-linear PDL values were used. Different loads were applied to a mandibular canine and first premolar to simulate orthodontic tooth movements. Two series of analyses were performed. The first series applied a constant force (100 cN) while varying the applied moment to examine the moment to force ratio. The second series varied the force levels from (0.5 to 200 cN) while keeping a continuous moment to force ratio. The centers of rotation were found to vary based on the moment-to-force ratio and the amount of force applied.

In another study, Cattaneo et al (20) described the orthodontic load transfer from teeth to the alveolus. The same material properties and methods were used as in the 2008 study.

Two anterior and two posterior teeth were subjected to an uncontrolled tipping force, a translation force, and a large occlusal force. Diagrams showing stress and strain distribution at the bone-PDL interface were generated. Results were contrary to the traditional view of tension and compression areas in the PDL when on a tooth under a translation force. The model revealed little compression and greater tension until the load reached a point where the tooth was nearly in contact with the bone.

Tanne et al (24) performed in vivo measurements of tooth displacements and used these data in a simplified 3-D finite element model (FEM). A periotest was used to measure the mobility of maxillary central incisors in fifty adults and fifty adolescents. Each tooth was measured five times, and the results were averaged. No differences were found between sexes, but a significant difference was noted between adults and adolescents. Young's modulus of the PDL was found to be higher in adults than in adolescents. A 3-D FEM of an maxillary right central incisor and surrounding periodontium was developed using generic anatomy. All materials were assumed to be isotropic and elastic. Using a 100g lingual force on the facial of the crown, PDL stress distributions were calculated using the 3-D FEM for three different Young's modulus values (two adult, one adolescent). The amount of tooth displacement did not vary with different mechanical properties of the alveolar bone. However, the Young's modulus of the PDL was found to be the most important determinant of instantaneous tooth movement. Contrary to Cattaneo, Tanne found significant compressive stresses were produced on the lingual side of the alveolar crest. These results were different possibly due to the assumption that the PDL was isotropic and elastic.

Jones et al (19) also conducted in vivo measurements of tooth displacement to evaluate the physical properties of the periodontal ligament. Ten young subjects with good

periodontal health were selected to represent typical PDL response to tooth loading. Laser measuring equipment recorded displacement of a central incisor in each subject while a precise, constant force was applied to the tooth over a specified time interval. Recordings were made over a 60 second interval consisting of 10 seconds pre-loading phase, 30 seconds under constant load, and 20 seconds of recovery. Teeth with tight inter-proximal contacts were excluded. Jones et al, then, constructed a 3-D model of a maxillary central incisor and applied values measured through in vivo experiments to the model. The 3-D FEM model included the single central incisor, surrounding PDL, and bone. The Young's modulus of the PDL was determined to be 1 N/mm2 with Poisson's ratio of 0.45, and the computed displacement matched the in vivo experimental results. A limitation of this study was that morphology of the teeth used in the 3-D model was based on a generic, ideal anatomy rather than the individual variations in anatomy of the 10 subjects. Another limitation was the use of unrealistic boundary conditions by fixing the PDL surfaces in all degrees of freedom. The study is based on a static analysis and is one of the few attempts to enter human *in vivo* data of tooth response to a load into a 3-D model.

Badawi et al (16) conducted laboratory tests using multi-axis force and moment transducers to simultaneously measure the load on each tooth. Fourteen aluminum cylinders were machined out of aluminum and placed in the appropriate maxillary arch position to represent teeth. Brackets were placed on the sensors and an archwire inserted. This allowed measurement of the all forces transferred to each tooth by different bracket-wire systems. The maxillary right canine was moved 4mm out of occlusion. 0.022-in slot Damon standard prescription brackets with 0.018-in copper-nickel-titanium wires were used to test elastomeric ties against passive ligation. The canine was moved to the zero position in

0.1mm increments while data was gathered at each movement. The data was interpreted with a 3-D, custom-made visualization software. Force magnitudes were found to be higher with conventional ligation using elastomeric rings than with the passive ligation. This research demonstrated the ability to measure the forces acting on orthodontically treated artificial teeth with activation of a continuous wire. However this state-of-the-art system did not take the PDL into account when measuring.

Ammar et al (25) attempted to demonstrate that 3-dimensional modeling with finite element analysis can be a clinical tool for treatment planning specific tooth movements. Specifically, analysis of a miniscrew used as skeletal anchorage in retracting a mandibular canine was conducted. An anatomically accurate 3-dimensional model was constructed by stacking 2-D slices to make a 3-D structure from cone-beam computed tomography scans. A virtual miniscrew was placed between the first and second molars to act as skeletal anchorage and a 200-cN tangential force was applied. A 100-cN distal tipping force was applied on the buccal surface of the canine. The point of application of the distal force was varied to simulate different lengths of the hook. Results showed that applying the horizontal retraction force near the center of resistance of the canine reduced stress in the PDL and gave a distal translation of the tooth. Critical stress was found in the top two threads of the miniscrew and the top 2.5mm of bone. Tightening loads were found to increase the stress on the miniscrew. An admitted limitation of this study was the omission of brackets and archwires.

In summary, most previous FEAs in orthodontics were limited by the omission of brackets and archwires. The force vectors were given relative to specified points. There were no simulations that used an archwire to apply stored force between multiple brackets.

The propagation of force through a continuous arch wire to the adjacent teeth represents true orthodontic biomechanics, which is yet to be investigated.

Continuous Archwire Model Using the "Birth and Death" Technique

Three recent studies have attempted to use continuous archwire for finite element simulation. Field et al (18) constructed a 3-D computer aided design (CAD) model of cortical bone, alveolar bone, enamel and dentin based on computed tomography images of an adult mandible. Brackets and a wire were added and the model was converted to a FEM. Both one tooth and three tooth segments were analyzed. Applied forces were directed normally to the brackets in a lingual and a distal direction to prevent disengagement of the wire and slot. Surface-to-surface contact was added to the three-tooth model to include interaction between teeth under the applied load. Results showed limited crown displacements in the multiple-tooth model and more displacement in the single tooth model. Differences were also seen in the compressive stress in the PDL. This was attributed to the additional stiffness of the model system caused by the adjacent teeth. Field stated that multiple teeth should be included in the model to accurately consider the force transmitted though contact points.

Sung et al (15) examined en-masse retraction with miniscrew anchorage using finite element analysis. Using a maxillary model with all upper teeth except the first premolars, the effect of anterior torque control was evaluated as a function of original anterior tooth axis, position, and vertical height of the miniscrew, length of retraction hook, compensating curve, and midline vertical traction. Virtual 0.019 x 0.025-inch and 0.016 x 0.025-inch stainless steel archwires were placed in crude blocks that represented slots of brackets. A compensating curve was simulated in the archwire by constructing a curved beam element.

The nodes connecting brackets and archwire were given translational degrees of freedom in the two flexural directions while being unconstrained in the axial direction. Friction between the wire and brackets was ignored. A 200-g retraction force was applied from the hook to the direction of the miniscrew. Results showed that retraction hook height and the compensating curve had limited effect. The 0.019 x 0.025-inch wire showed less incisor tipping than the 0.016 x 0.025-inch wire. Higher miniscrew location to longer retraction hooks placed the direction of the force closer to the center of resistance, resulting in less distal tipping of the anterior teeth. Since their model included archwires and crude brackets, this study is one of the first finite element models to include the force transfer between the bracket system and accurate dentition. Unfortunately, all the interfaces were rigidly bonded that may yield unreal predictions.

Kim et al (26) used a finite element model to evaluate the retraction arm position and length to achieve controlled en masse retraction of anterior teeth. In this model, crude brackets and an archwire were placed on six upper anterior teeth and accurate surrounding anatomy. Virtual 0.021 x 0.025-inch stainless steel archwires were placed in 0.022-inch slot brackets. A coefficient of friction between the archwire and brackets was defined as 0.2. The power arm was connected to the archwire and considered one object. A 150-g force was applied at different angles to a retraction hook that varied in length (3 to 11 mm) and location on the archwire (between lateral incisor and canine or between canine and first premolar positions). A series of points down the long axis of each tooth was measured to allow differences in tooth displacement to be evaluated. Results showed that the length of the retraction arm must be increased as its position on the archwire is moved from the lateral

incisor to the premolar to produce a translated movement. The bracket system interaction with the dentition used in this finite element model is similar to that of Sung et al (15).

The aforementioned model considered interaction of neighboring teeth and archwire connectivity. Nevertheless, the assumption of beam elements and rigidly bonded interfaces decreased accuracy of their model prediction. Previous orthodontic FE models failed to incorporate accurate human anatomy, multiple teeth, and complete bracket-wire systems all in one system. A new FE model with multiple teeth and capability of exert unloading force (storage energy) of the archwire is needed.

In the present study, the anatomy of a maxilla and dentition, including enamel, dentin, pulp, PDL, lamina dura, trabecular and cortical bone, was created from CBCT and micro-CT data. CAD-generated braces were bonded to the enamel of each tooth and a rectangular archwire was tied with ligature wires and in contact with braces. The intrusive step bend on the wire was activated by applying element "birth and death" behavior (ANSYS13.0) to allow both loading and unloading force acting on the brackets. This birth-death function of finite element analysis software has yet to be used in published orthodontic literature.

Central Hypothesis

It was hypothesized in the present study that the deactivation (unloading) of a continuous archwire can be effectively simulated by using the "birth and death" model, and biomechanical behaviors of lingual versus labial bracket system differ during the archwire deactivation stages.

Specific aims include:

1) Develop complete labial and lingual bracket-wire systems on accurate anatomy including multiple teeth, and validate this model by comparison to a stainless steel model of all the structures.

2) Analyze forces transferred throughout the dentition and surrounding structures by clinically realistic wire bends using the birth-death technique.

3) Evaluate clinically relevant biomechanical differences between labial and lingual bracket systems through an intrusive step bend.

III MATERIALS AND METHODS

To achieve the Specific Aim 1, we constructed an orthodontically accurate FE model combining: an anatomical tooth-bone model and a CAD bracket system model. Two sub-models were generated based on material definitions. One was assigned stainless steel for all structures and the control was assigned correct material properties for each structure. The control model was compared to the steel model to examine the importance of PDL and bone. The null hypothesis for this aim is that there are no differences in mechanics between the anatomically accurate model and the all steel model.

Tooth-Bone Model Construction

A three-dimensional human maxilla computer model constructed at UNC Department of Orthodontics was modified for use in this study. 0.5 mm 2-D, cone beam (CBCT) slices of a human dentate maxilla were used as templates for construction of the bone model. By sequentially stacking the 2-D slices, a 3-D model of cortical bone, lamina dura and sinuses was created with the Computer-Aided Design (CAD) software Solidworks (Solidworks Corp., Concord, MA, USA). The dentition was built from micro-CT data (micro-CT40, Scanco Medical, Basserdorf, Switzerland; courtesy of Paulo Cattaneo, Dept. of Orthodontics, Royal Dental College, University of Aarhus). The dentin, enamel and pulp were built in Solidworks using the CT slices as templates. The 0.25 mm thick PDL and 0.5 mm thick lamina dura were added around each tooth. The teeth were placed into the bone model and the overlapping area was subtracted from the bone. The lamina dura of each tooth was merged with the surrounding cortical bone to unify the model.

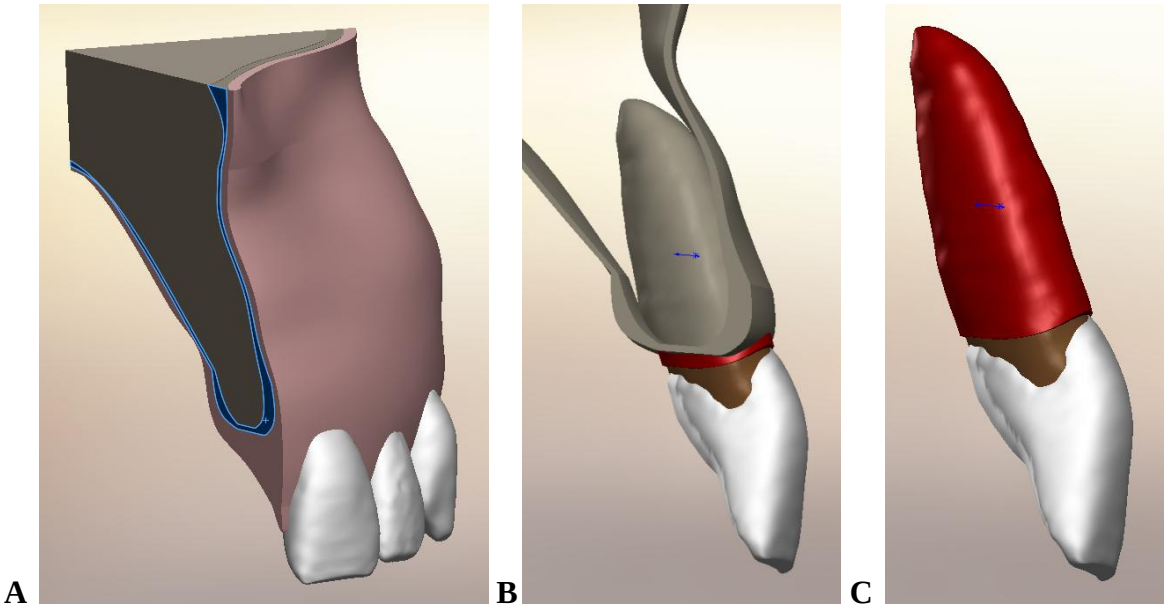

Figure 2. A, Sectioned model with cortical bone (blue); **B,** Lamina dura and cortical bone with gingival and trabecular bone transparent; **C,** central incisor with periodontal ligament.

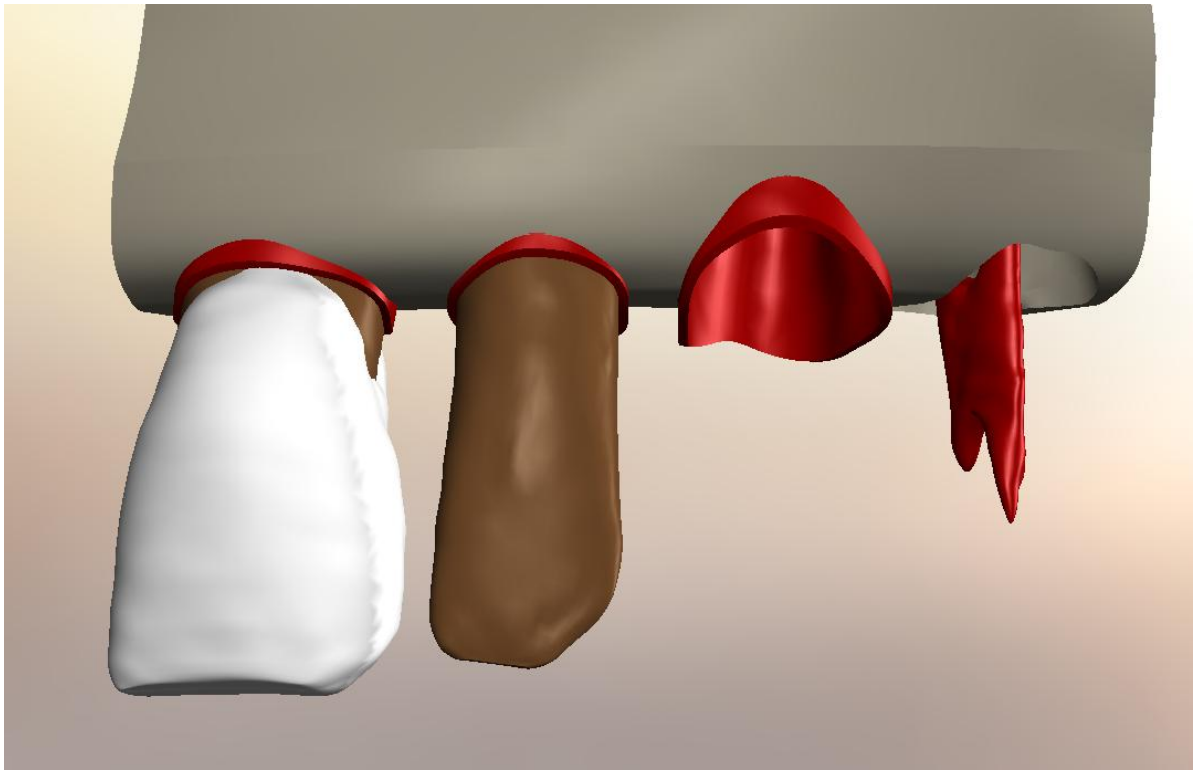

Figure 3. Dissected model shows a complete central incisor, lateral incisor dentin, canine periodontal ligament, and first premolar pulp.

A 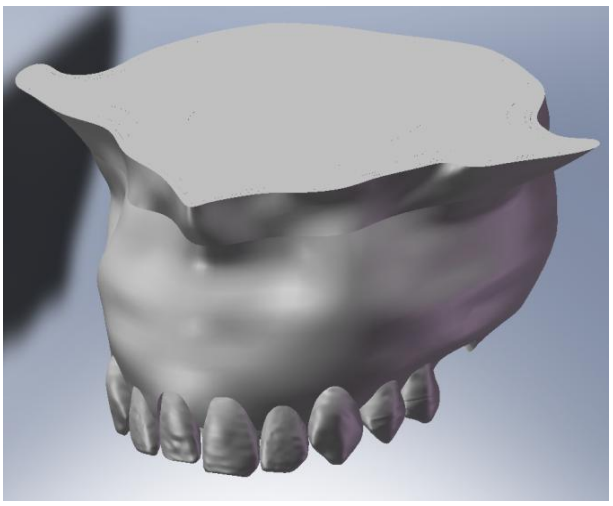 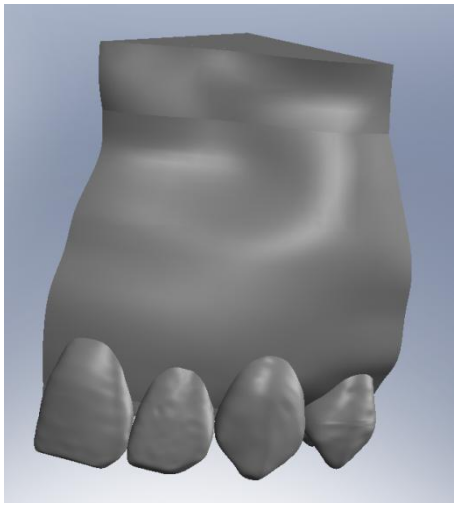 B

Figure 4. A, Complete maxilla model; **B,** sectioned model with central incisor, lateral incisor, canine, and premolar.

The model was sectioned from the interproximal region between the maxillary central incisors as the mesial boundary, to the interproximal region between the maxillary right first and second premolars as the distal boundary. The model included the occlusal surface of each tooth to the inferior part of the right maxillary sinus and palate.

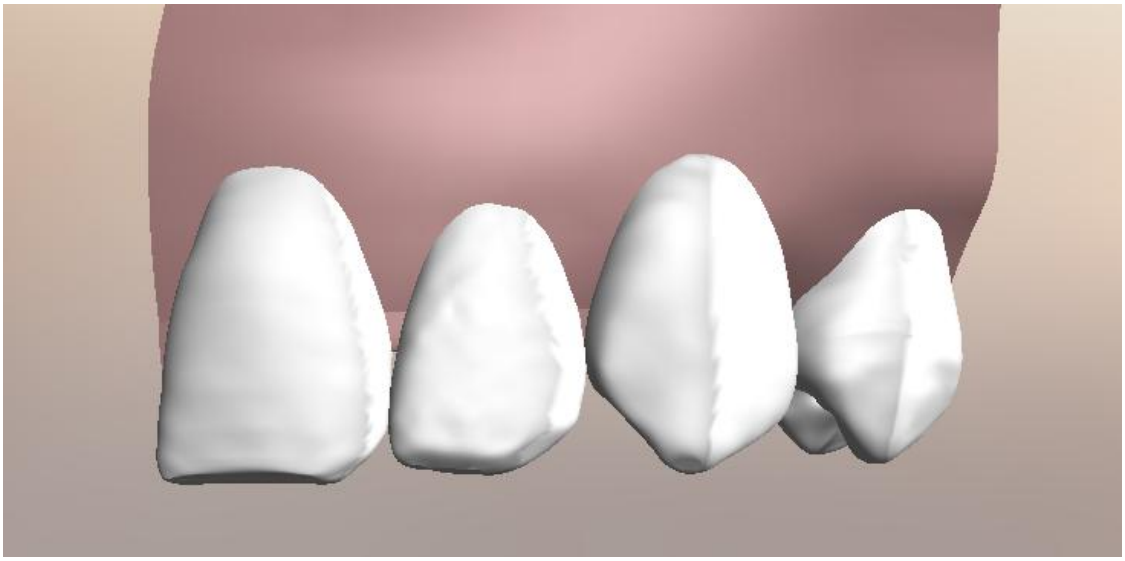

Figure 5. Complete, sectioned model includes upper left central incisor, lateral incisor, canine, and first premolar. Model is ready for bracket placement.

Lingual Bracket Construction

The Incognito Bracket System was used to represent the lingual appliance. This system utilized a digital scan of the dentition to design and optimally place virtual brackets on the digital teeth. The aforementioned UNC 3-D model was submitted to the manufacturer. 3-D models of Incognito lingual brackets were adapted to the UNC teeth model. The stereolithography (stl) CAD design of virtual brackets was provided by the manufacturer for inclusion in the model.

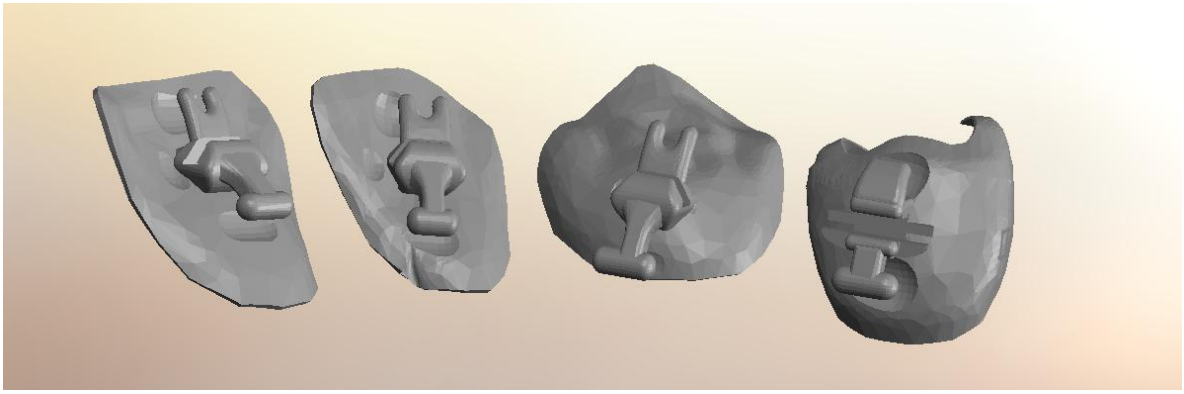

Figure 6. Incognito brackets were custom designed for the anatomy of the model and provided by the manufacturer. Brackets include (from left to right): maxillary left central incisor, lateral incisor, canine, and first premolar.

The lingual brackets were placed on the teeth so that the gingival bases of the slots were on the reference plane while the internal surfaces of the brackets minimally overlapped the lingual tooth surface. No internal gaps were left between the enamel and bracket surface.

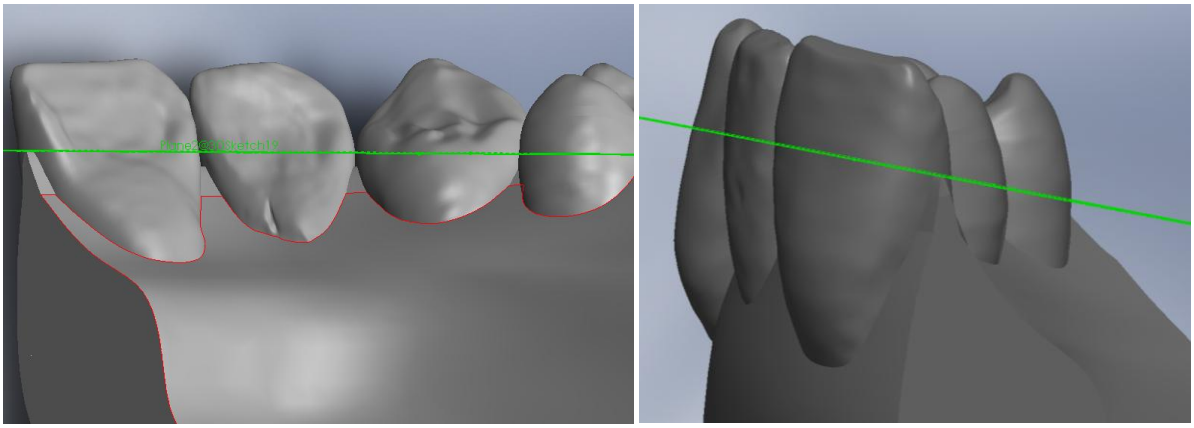

Figure 7. To ensure that the palatal surface of each bracket slot was on the same plane, a reference plane parallel to the occlusal plane was created. Two aspects of the plane are shown.

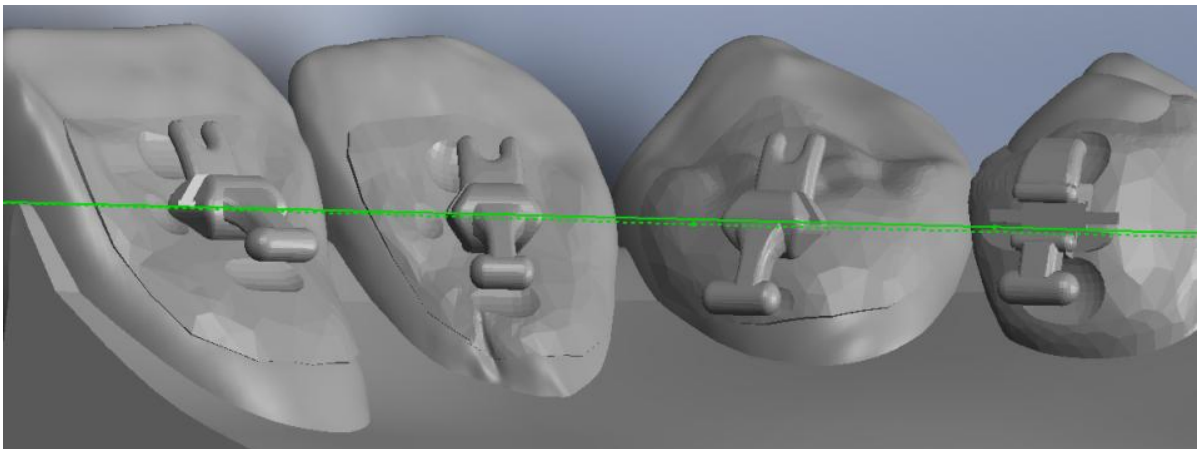

Figure 8. Lingual brackets were positioned with the gingival base of the slots on the reference plane. Each bracket minimally penetrates the enamel with no gaps remaining between the tooth and proximal bracket surface.

A Boolean operation subtracted the overlapping part of the bracket base with the tooth to ensure a smooth bracket surface interfacing the lingual surface of the tooth.

A 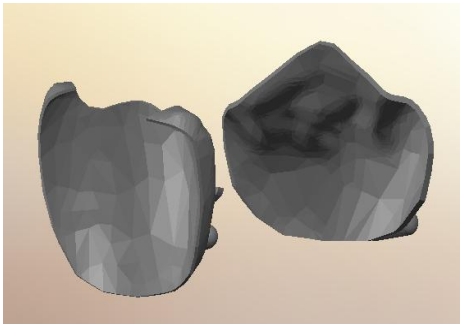 B 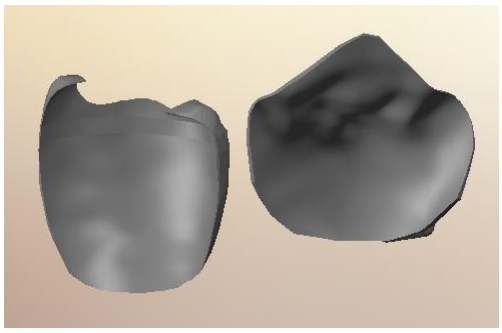

Figure 9. Internal surfaces of the canine and first premolar lingual brackets. The surfaces were: **A,** rough when provided by the manufacturer and were then **B,** smoothed by the Boolean function to ensure a smooth contact with the enamel.

The buccolingual slot width of the virtual brackets was 0.0165 inches as provided by the manufacturer, and was increased to 0.0183 to accommodate a 0.018 x 0.018 inch wire with two degrees of play.

A 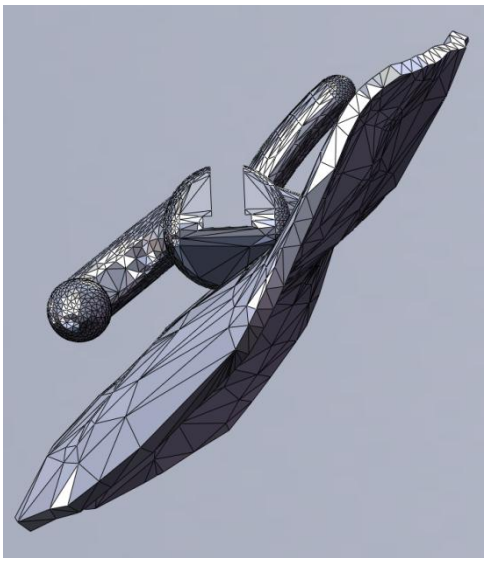 B 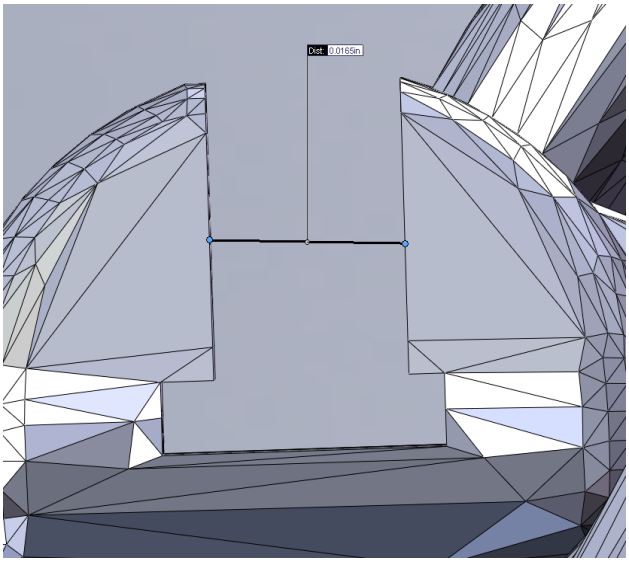

Figure 10. **A,** Central incisor lingual bracket viewed from the distal; **B,** Close up view of the same bracket slot that was widened from 0.0165 inches to 0.0183 inches to accommodate an 0.018 inch archwire.

Labial Bracket Construction

3D CAD models of 0.022 inch slot, standard labial brackets were provided by Dr. Clarke Stevens of WildSmiles. The bracket base and slot assembly were separate when delivered by the manufacturer (Figure 11).

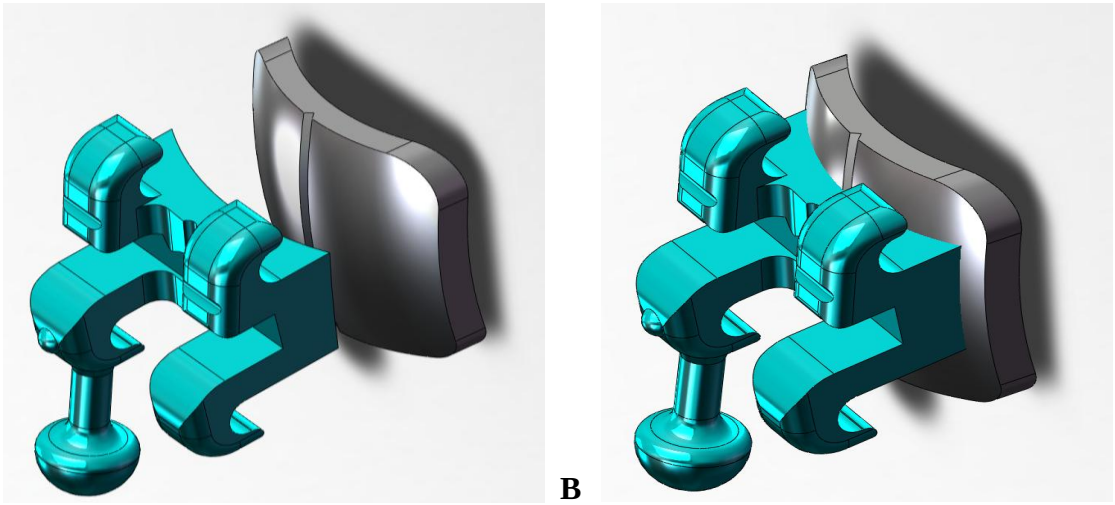

Figure 11. A, Labial bracket parts were provided by the manufacturer; **B,** Assembled 0.022 inch slot, labial bracket.

The bracket bases were placed in a way that they minimally overlapped the facial tooth surface. The elimination of the gaps between two bodies was included to prevent possible problems achieving divergence during the finite element solution. To place the bracket assemblies on the bases ensuring all slots remained on the same plane, a reference plane that was parallel to the occlusal plane was defined. The slot assemblies were placed on the bracket bases with minimal overlap while keeping the occlusal surface of the bracket slot on the reference plane (figure 12).

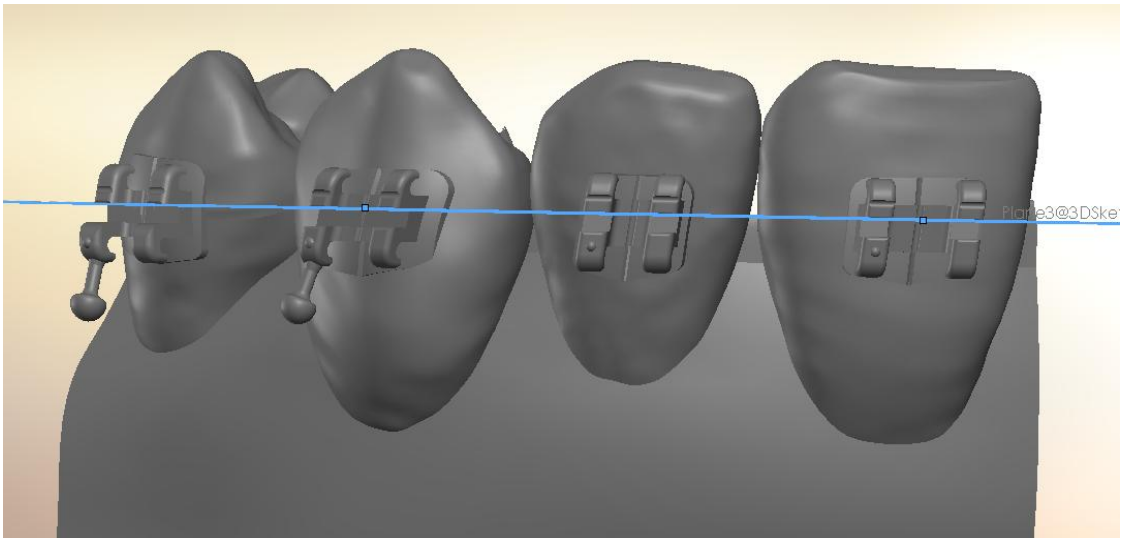

Figure 12. Assembled 0.022 inch slot, labial brackets placed with the incisal slot surface on the reference plane. Each bracket minimally penetrates the enamel with no gaps remaining between the tooth and proximal bracket surface.

Wire Construction

Specific Aim 2 was an attempt to simulate orthodontic archwires unloading force on the brackets. To achieve this aim, the continuous archwires with intrusion bends were first constructed and inserted into the tooth-bracket model (Aim 1) to complete the CAD model. This combined CAD model was then converted into a finite element model to compute deactivation force of the continuous archwire.

Lingual Wire Construction

A 0.018 inch by 0.018 inch lingual wire that follows the construction technique used by the Incognito system was created in Solidworks. Starting from the gingival and proximal corner of the bracket, the portions of wire that engage the bracket slot were assembled first. These sections of straight wire were extended beyond the slot by one third of the width of the slot at each end. Bends made over 1.0mm sections of wire were placed at either end of the extension out of the slot. A straight piece of wire connected the two bent sections making

one continuous section of wire. Each interproximal section had two first order bends. The continuous wire was placed in the model so that it passively engaged each slot.

Labial Wire Construction

A 0.019 x 0.025 inch archwire was built for the labial bracket system. Starting from the occlusal and proximal corner of the bracket, the portions of wire that engage the bracket slot were assembled first (Figure 13). These straight, slot-engaging segments were extended 0.1 mm beyond each end of the facial slot. The interproximal sections were constructed to make a curved archform (Figure 14). Bends were made over 1.0mm sections of wire and placed interproximal to the central and lateral incisor as well as the canine and lateral incisor (Figure 15). The interproximal segments were connected to the slot-filling segments to create a continuous wire (Figure16).

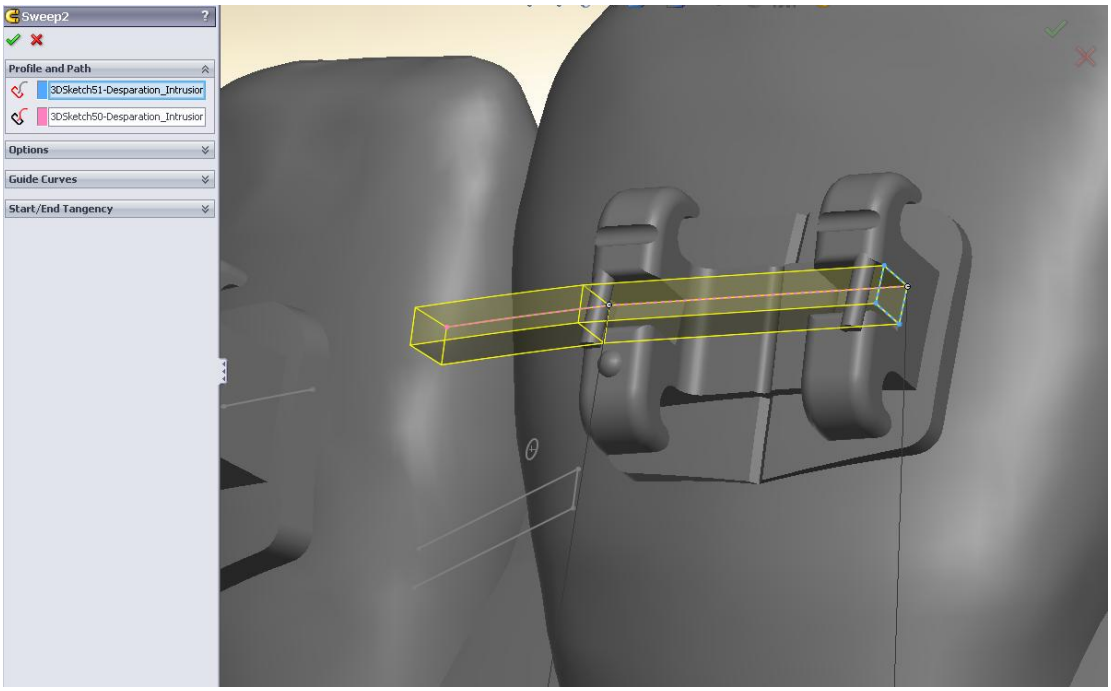

Figure 13. Straight, slot-engaging segments of wire extend 0.1mm beyond the edge of the brackets. Interproximal segments that followed the archform curvature were connected to these segments.

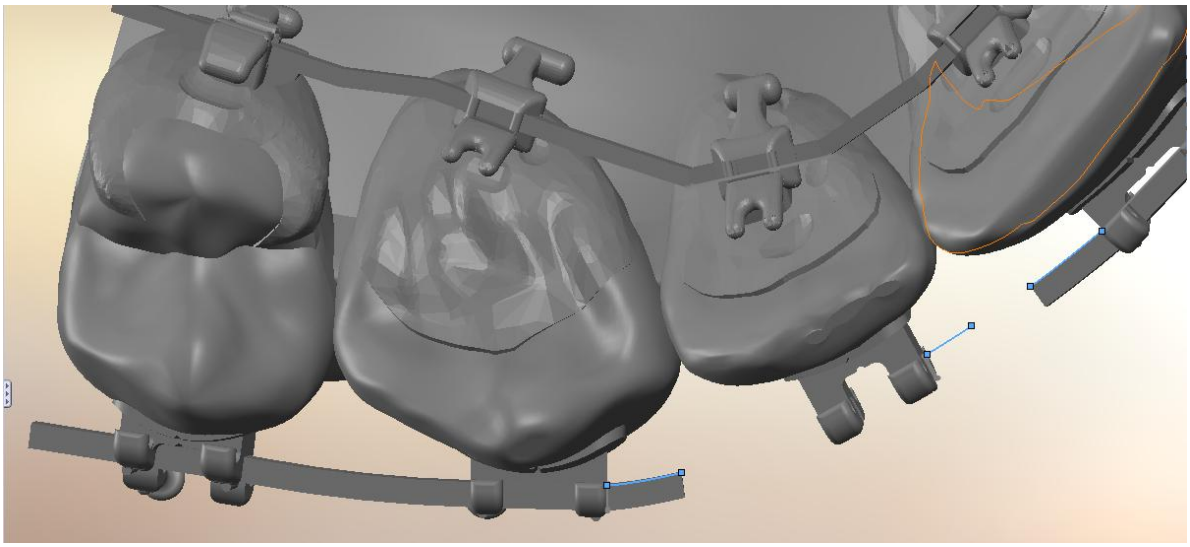

Figure 14. Occlusal view of labial archwire assembly. Interproximal segments that followed the archform curvature were connected to these segments.

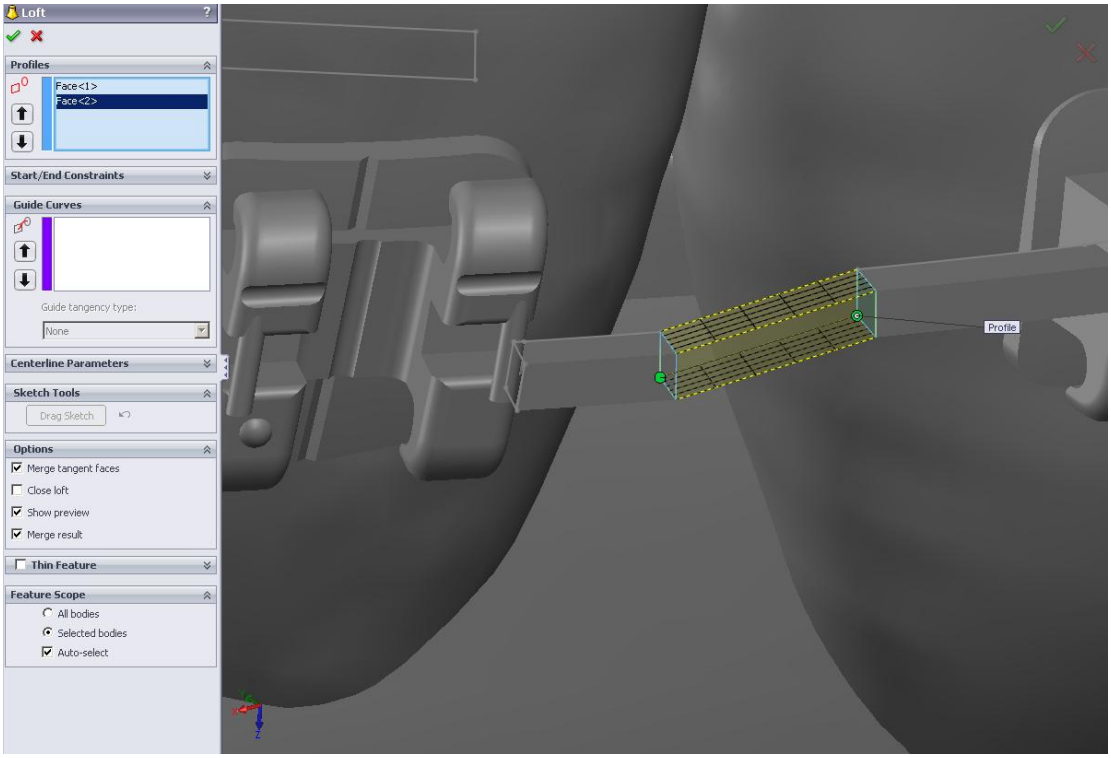

Figure 15. Bends were formed over a 1.0 mm segment of wire using the Solidworks loft function.

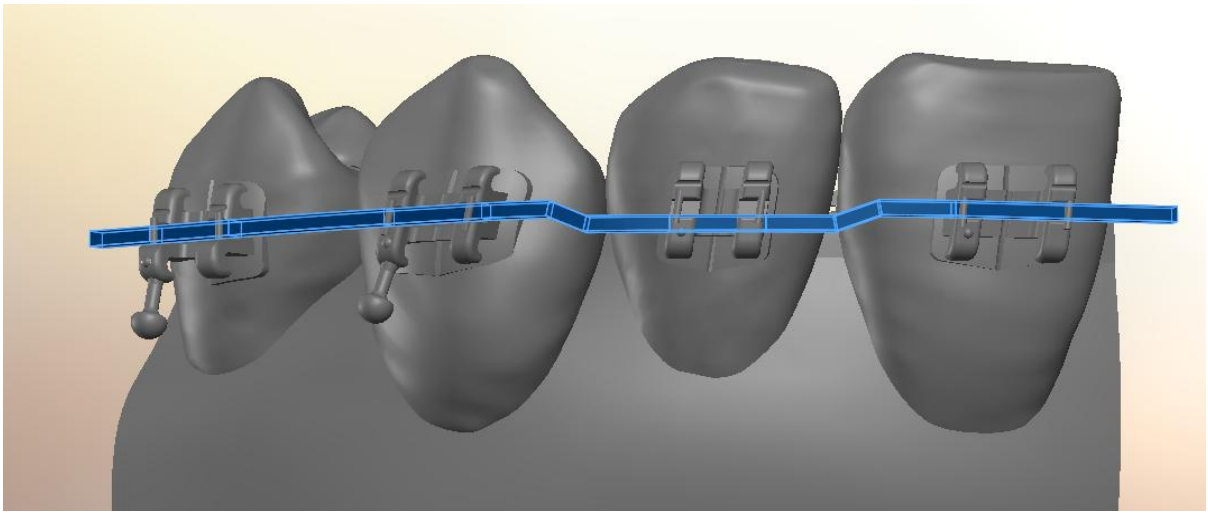

Figure 16. The interproximal segments were connected to the slot-filling segments to create a continuous wire.

Using the passive wire as a starting point, a 0.5 mm intrusion bend was made at the lateral incisor position. Bends were placed in the adjacent interproximal areas for the facial wire. For the lingual wire, the bends were placed in the same location as the first order bends. Interproximal wire lengths and bracket widths are listed in Table 1.

Table 1. Wire Lengths and Bracket Widths (mm)

	Labial	Lingual
Mesial end-UL1	3.39	3.14
UL1 Bracket	3.82	2.50
Interproximal UL1-2	5.51	4.65
UL2 Bracket	3.00	2.10
Interproximal 2-3	5.19	4.69
UL3 Bracket	3.43	2.10
Interproximal UL3-4	5.50	4.09
UL4 Bracket	3.15	3.20
UL4-distal end	2.38	1.85

To simulate ligature wires that hold the archwire inside the bracket slot, two 0.010 inch cylinders were added at either end of the slot opening (Figure 17). The ligatures were placed to touch but not overlap the archwire. These were combined with the brackets to form one body.

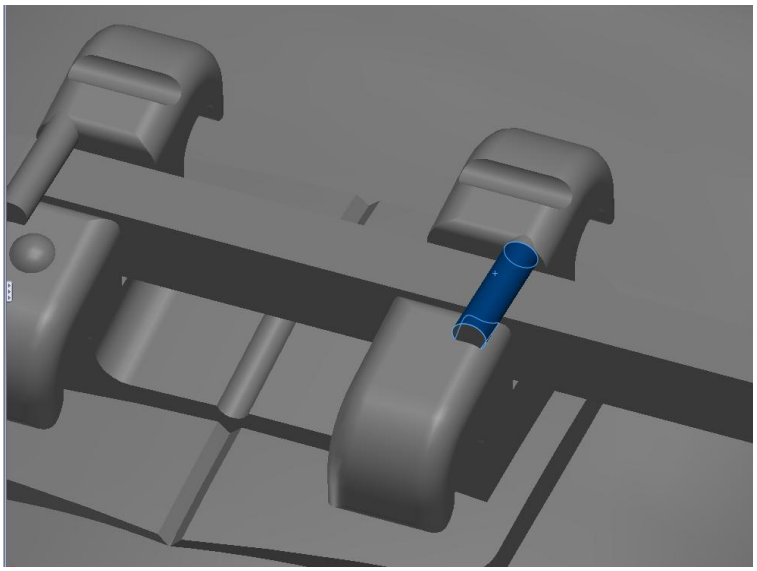

Figure 17. Two 0.010 inch cylinders were placed on each bracket to prevent the wire from disengaging from the slot.

The complete CAD model was established and the solid body information was saved into IGES file format using SolidWorks software (Solidworks Corp., Concord, MA, USA).

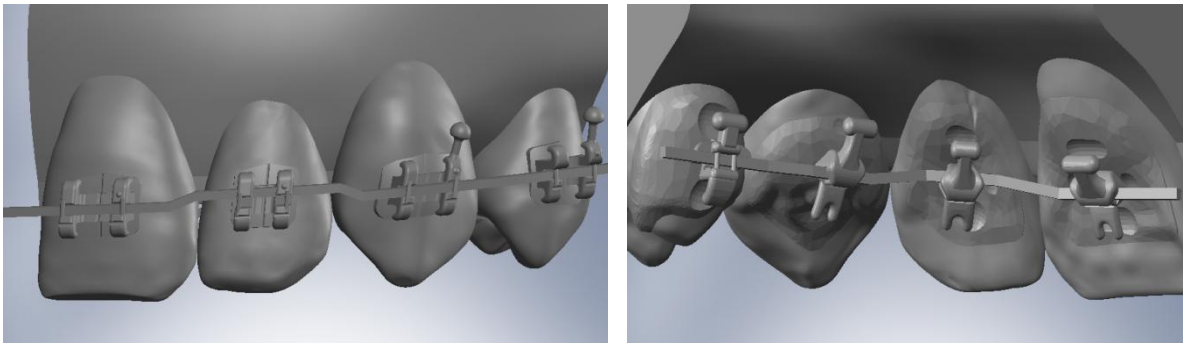

Figure 18. Final assembled Solidworks models ready for conversion to ANSYS for simulation.

Finite Element Model with "Birth and Death" Function

IGES file format of the model was loaded into ANSYS 13.0 Workbench (Swanson Analysis Inc., Hutson, PA, USA). The assigned material property definitions are listed in Table 2. Using Design Modeler mode of ANSYS, the solid parts (e.g., bracket, ligature wire, enamel, dentin, pulp, PDL, lamina dura, trabecular and cortical bone) were merged. The archwire was not merged with the model for meshing. Instead, the archwire was meshed separately, and the nodes in the archwire did not bind to the nodes in the brackets. Interfaces between different materials were rigidly bonded using the penalty method. The model was meshed and consisted of 238758 nodes and 147747 elements. All bodies had a tetrahedral mesh, except the archwire, which had a swept mesh. The model was fixed at the ends of the archwire and at the cortical and trabecular bone at the midline and distal to the first premolar.

Table 2. Material Properties

	Poisson's Ratio	Young's Modulus (Pa)	Bulk Modulus (Pa)	Shear Modulus (Pa)	Density (kg/m^3)
Enamel	0.41	8.00E+10	1.48E+11	2.84E+10	2000
Dentin	0.31	1.80E+10	1.58E+10	6.87E+09	1600
Pulp	0.30	1.75E+08	1.46E+08	6.73E+07	1000
PDL	0.30	1.75E+09	1.46E+09	6.73E+08	1000
Cortical Bone	0.31	1.37E+10	1.20E+10	5.23E+09	1600
Trabecular Bone	0.30	1.37E+09	1.42E+09	5.27E+08	1400
Gold	0.30	1.00E+11	8.33E+10	3.85E+10	19300
Steel	0.30	2.00E+11	1.67E+11	7.69E+10	7850

To simulate the deactivation force of the archwire, an intrusive bend of the labial archwire was used and the Newton-Raphson procedure, called “Birth and Death” in ANSYS, was performed to test convergence of the solver. Two load steps were executed in the solution process. In load step 1, the elements in the contact areas between the bend portion of wire and the overlapped the lateral incisor bracket were intentionally ignored or “killed” also known as death. Step 1 allowed the engagement force to be simulated and the solution of this step was then restarted as the initial condition of load step 2 of solution. During step 1, the wire segment to be placed in the lateral incisor slot was then displaced far enough to allow the wire to fit into the slot with no overlap. This caused the engaging force to be applied by the wire to the central incisor and canine brackets. This displacement, in effect, loaded stored energy in the wire and adjacent teeth. In load step 2, the virtual contact areas in the lateral incisor bracket were then re-activated – “alive”, also known as birth. This is the “Birth and Death” function that allows the software to activate contact areas at a later step in the simulation. Then the displacement was released. As the wire rebounded towards its

original form, it contacted the lateral incisor bracket causing the stored energy to be released by displacing the lateral incisor. The convergence was checked.

Three models were constructed with this technique. For specific aim 1, two geometrically-identical, labial-bracket models were analyzed. One had correct material properties assigned and the other had all bodies assigned stainless steel. In specific aim 3, the labial bracket model was compared with a lingual bracket model. Both models had correct material properties assigned.

Clinical Application – Incognito Lingual Biomechanics

The above "Birth and Death" finite element model was applied to investigate Incognito lingual biomechanics. The 0.5 mm step intrusive bend (0.018 by 0.018 inch archwire) acting on the maxillary lateral incisor was simulated using Incognito bracket system. Contact interfaces with a coefficient of friction of 0.30 were assumed at the interface between the wire and brackets. All materials were assumed to be isotropic and linear elastic. The static equilibrium equations were solved under large displacement assumption. The activation of storage energy via the archwire was the same as described above. Deformation of the system was evaluated to confirm the validity of the solution. Deformation vectors were plotted to determine the center of rotation of the lateral incisor.

Analysis

Stress fields were analyzed to investigate effects of an intrusive bend on the PDL and surrounding bone. Areas of von Mises, maximal (tensile), and minimal (compressive) stresses were visualized to see if they are consistent with the clinically observed regions for bone resorption and formation. The peak tensile, compressive and von Mises stresses were computed and their locations were identified.

Regions of interest that were focused upon included the periodontal ligament, adjacent bone, tooth surfaces, interface between the wire and bracket, and any other regions which result in stress patterns that differ noticeably from the labial bracket model described above. Numerical analysis of deformation and stress fields were conducted at various points throughout the model. Eleven probes were placed on the facial surface of the lateral incisor to evaluate deformation at specific locations. Stress patterns and distributions were compared visually by setting the same scale to both simulations and viewing the solution display from the same angle.

IV RESULTS

Aim 1. Advanced Finite Element Model

The goal of placing complete labial and lingual bracket-wire systems on accurate anatomy, named the PDL model in the following text, including multiple teeth was achieved. The conversion from a 3D Model in Solidworks to ANSYS for finite element discretization resulted in a conformal mesh. Using the example of the labial bracket system, the solid mesh model was solved with convergence.

Both labial models (stainless steel and PDL) were run with a 0.5mm intrusion step, and vector plots of total deformation showed the general location of the center of rotation for the lateral incisor for both models (Figures 20 and 21). The position of the centers of rotation varied depending on the model used. The lateral incisor center of rotation in the PDL model was on the mesial side of the pulp and 4.83mm from the apex. When assigned stainless steel material properties to all structures, the center of rotation changed to a location buccal to the root and between the roots of the lateral incisor and canine. The total displacement (0.0309 mm) of the lateral incisor edge in the PDL was 4.5 times greater than that in the all steel model (0.00689 mm). The displacement field of the lateral incisor in the PDL model gradually decreased from the incisal edge toward the root tip while the all steel model showed more concentrated deformation in the crown with abrupt decrease from cervix to the root tip.

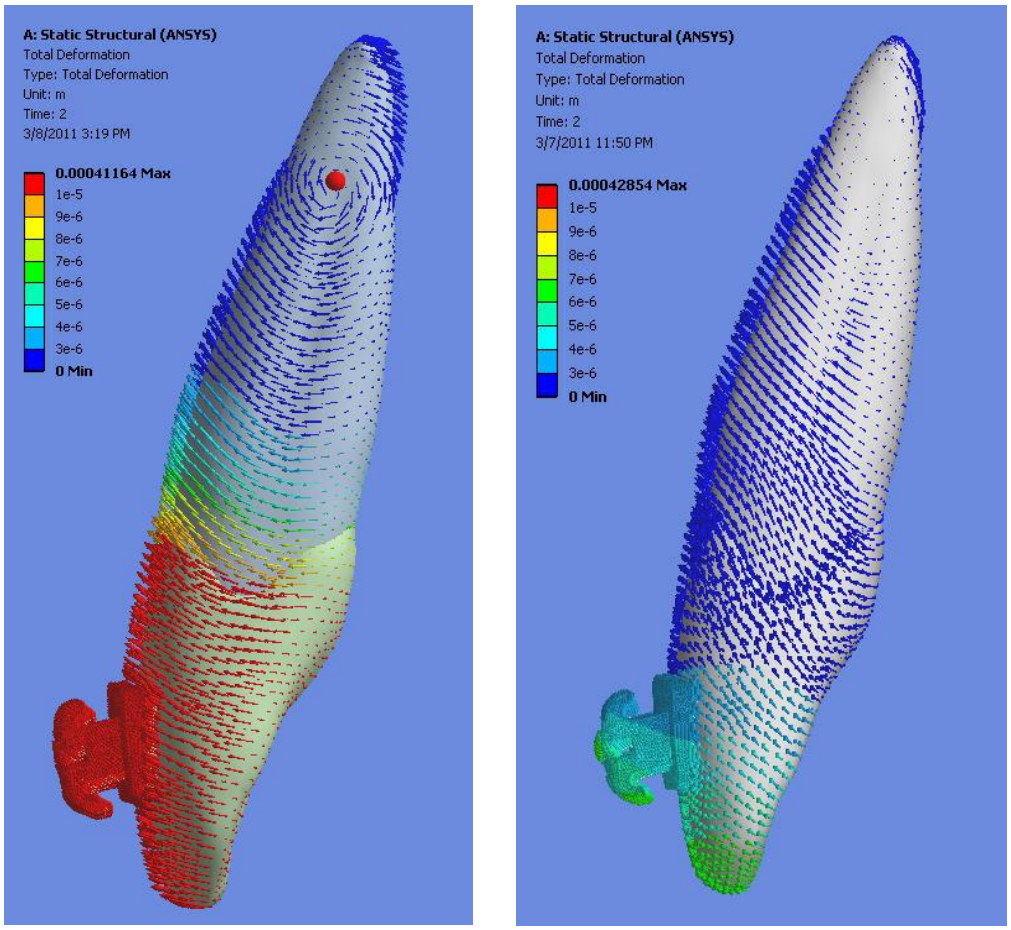

Figure 19. Total deformation of the lateral incisor with correct material properties assigned (left) versus with all structures assigned stainless steel material properties (right). Bone and surrounding structures are transparent for display.

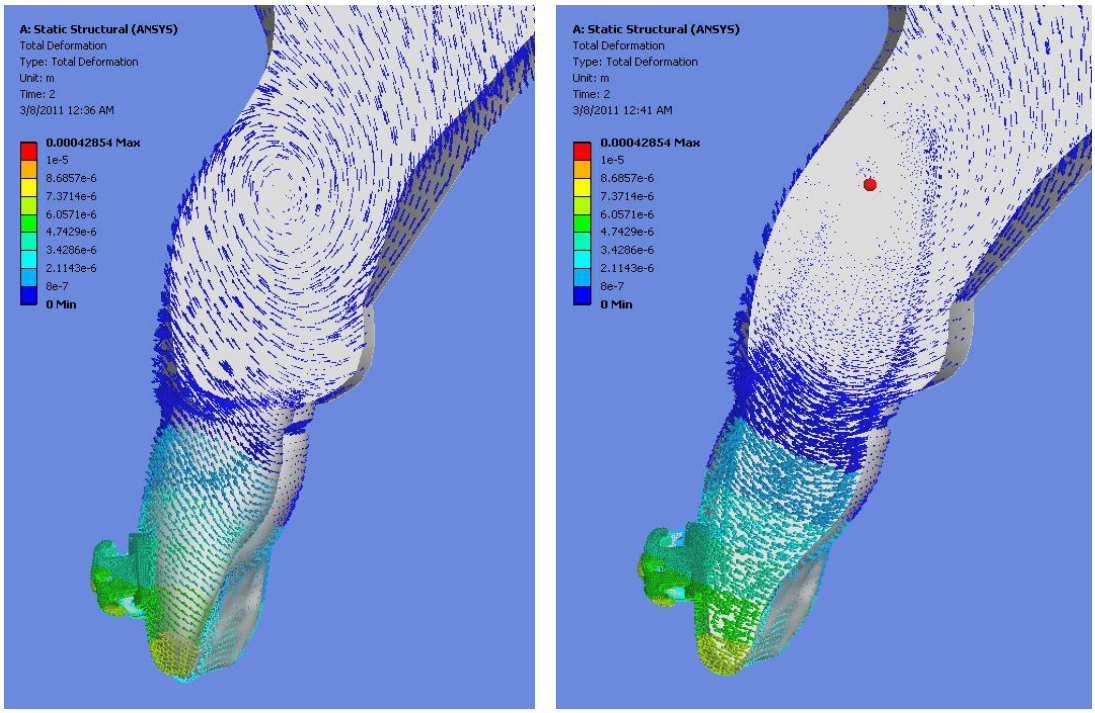

Figure 20. Location of the center of resistance in the stainless steel model is seen in the display of total deformation when the model sectioned between the lateral incisor and the canine (right) and sectioned through the lateral incisor (left).

Table 1 displays the reaction force at the bracket-wire interface in Newtons. Forces are higher at each bracket in the stainless steel model than in the PDL model. Peak compressive stress was located at the lateral incisor archwire-bracket interface and values were 2170 MPa for the PDL model and 2219 MPa for the stainless steel model.

Table 3. Bracket-Wire Reaction Force (N) for PDL and Steel Models

	U1 Force	U2 Force	U3 Force
PDL Model	19.1	21.9	19.9
Stainless Steel Model	20.3	24.5	23.0

On both stainless steel and PDL models, stress concentration was seen in the enamel of adjacent teeth in the interproximal contact areas indicating a transfer of force between the teeth (Figure 21). Such contact force could not be included in single tooth finite element models reported in the literature.

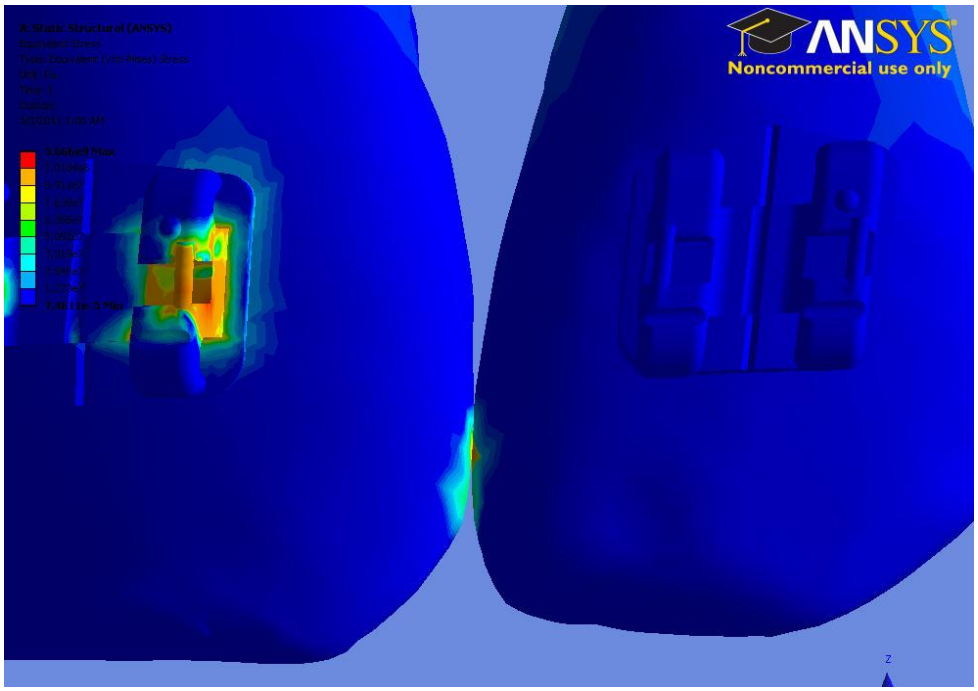

Figure 21. Stress transfer between adjacent teeth is seen in the color map of equivalent stress in the interproximal area between the central and lateral incisors.

Aim 2. Birth-Death Technique

The "birth-death" technique effectively simulated loading the archwire, with a clinically-realistic step bend, into the bracket slots. Static structural solutions at two loading steps (element kill and element birth) were found, and results were generated for maximum and minimum principal elastic strain, equivalent elastic strain, maximum and minimum principal stress, equivalent (von-Mises) stress, and total deformation.

The birth-death technique included three steps: 1) de-activation of the contact (element kill) and displacement of the archwire 2) activation of the contact (element birth)

between the archwire and lateral bracket 3) removal of the displacement of the archwire (unloading). Figure 22 shows the stress distribution in the wire and brackets early in step one. Before the contact areas were activated in the lateral incisor bracket, displacement of the wire placed stress on the canine and central incisor brackets (Figure 23). Because the elements were deactivated, no stress was revealed in the bracket of the lateral incisor. Once the contact was re-activated (step 2) and the displacing force on the wire was released, the stress increased in the lateral incisor bracket and decreased in the adjacent brackets. This process was clearly shown in simulation video of the loading the wire being loaded into the brackets. After the displacement force was entirely removed, stress levels (Figure 24) and force levels (table 4) were higher in lateral incisor bracket than the central incisor or canine brackets.

Table 4. Bracket-Wire Reaction Force (N) During Birth-Death Technique

	Central Incisor	Lateral Incisor	Canine
Step Two	40.1	0.0	18.8
Step Three	19.1	21.9	19.9

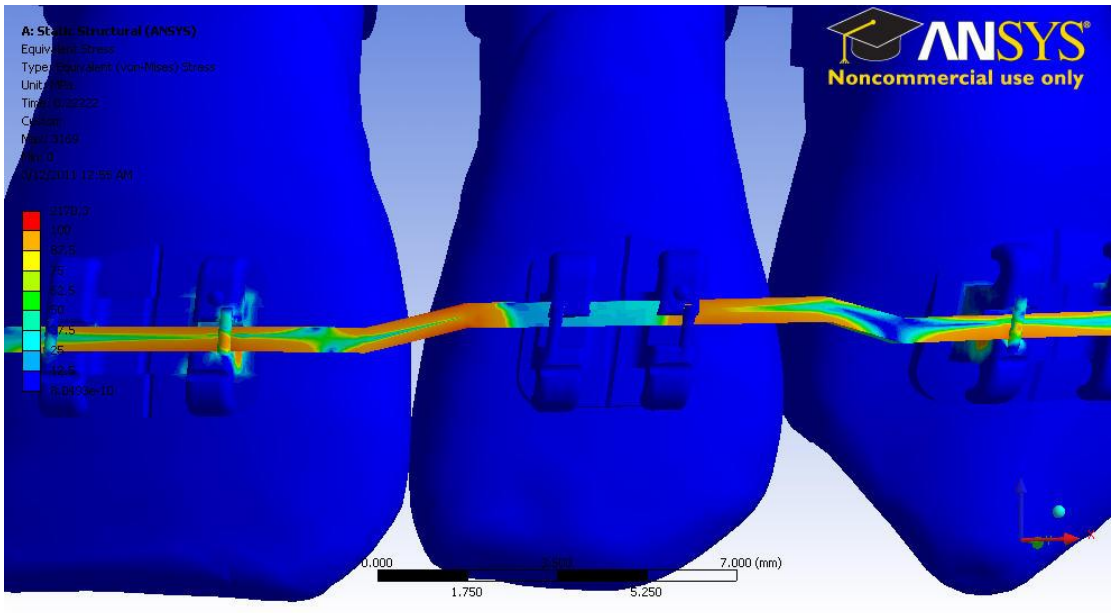

Figure 22. Equivalent (von-Mises) stress is shown at the first step of the birth-death technique when the wire is being displaced into the lateral bracket slot.

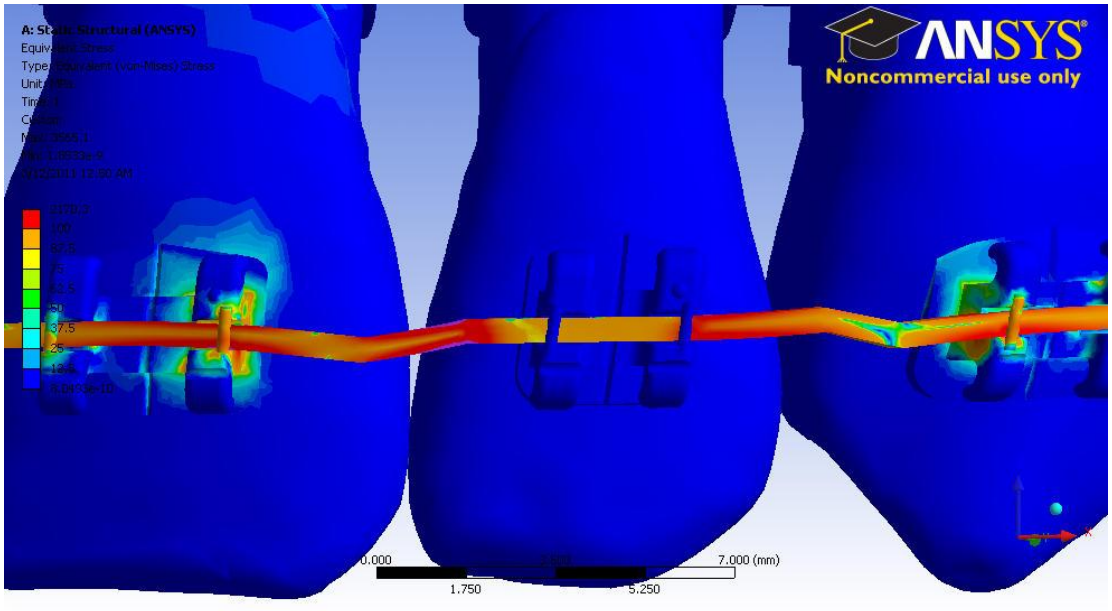

Figure 23. Equivalent (von-Mises) stress is shown just before the second birth-death step where the contact is activated. High stress is seen in the central incisor and lateral brackets.

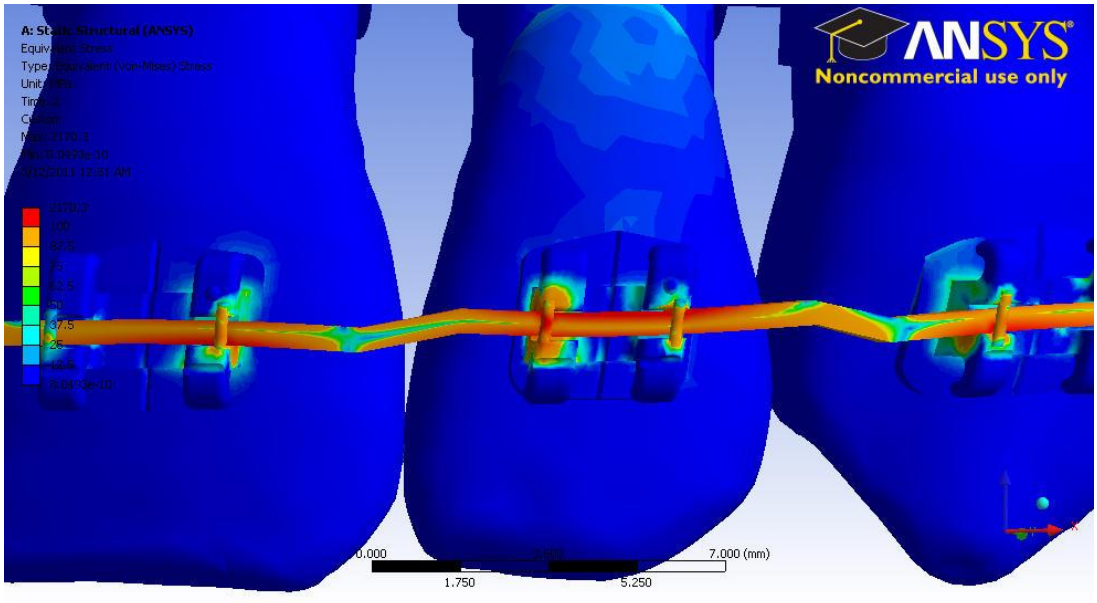

Figure 24. Equivalent (von-Mises) stress at the end of the simulation after the lateral incisor to wire contact has been activated and the wire has rebounded towards its original position.

As shown in Figure 25, the wire deformed from a passive configuration (black line) to the active form (gold colored wire). The maximum distortion area, as expected, is at the lateral incisor area. Figure 26 depicts stress distribution as a color map on the wire. The gradient of color represents equivalent stress in Pascals. The stress field in the bracket-wire system is separated to show compression (Figure 27) and tension (Figure 28) as a color map.

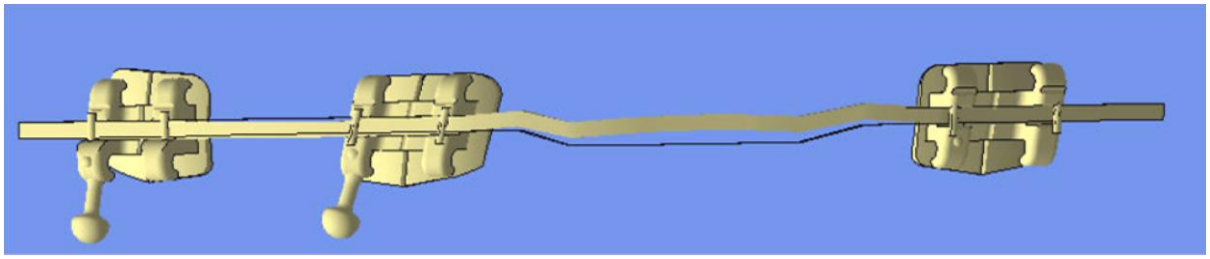

Figure 25. Deformation of the 0.019 x 0.025 inch stainless steel archwire. The line shows the original form. The solid structure displays the wire at the end of the simulation once the wire is engaged in the lateral incisor bracket.

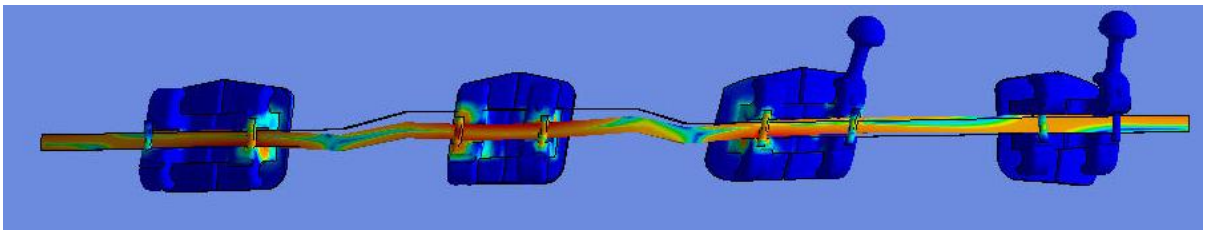

Figure 26. Equivalent (von-Mises) stress distribution of the 0.019 x 0.025 inch stainless steel archwire.

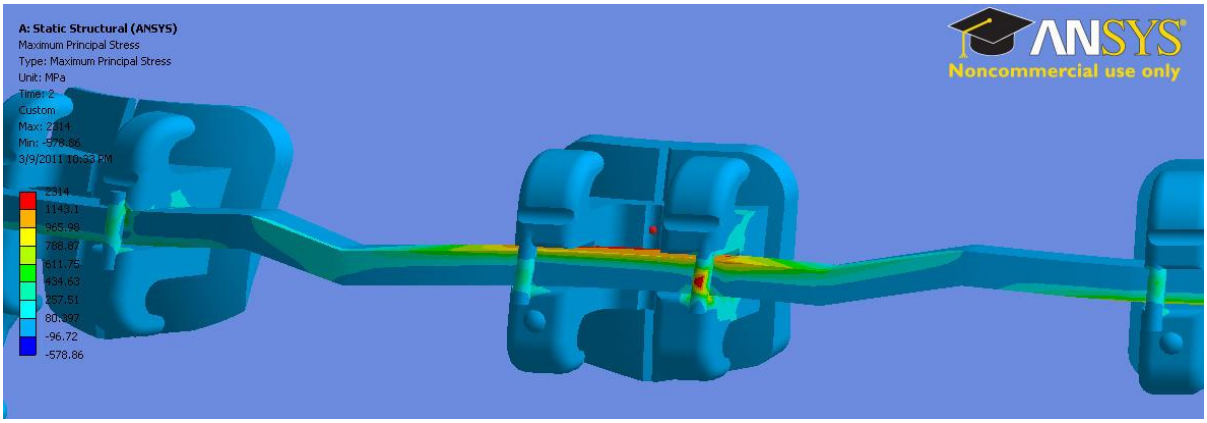

Figure 27. Compression (maximum principal stress) distribution of the 0.019 x 0.025 inch stainless steel archwire activated with a 0.5 mm intrusive step into the lateral incisor bracket (middle).

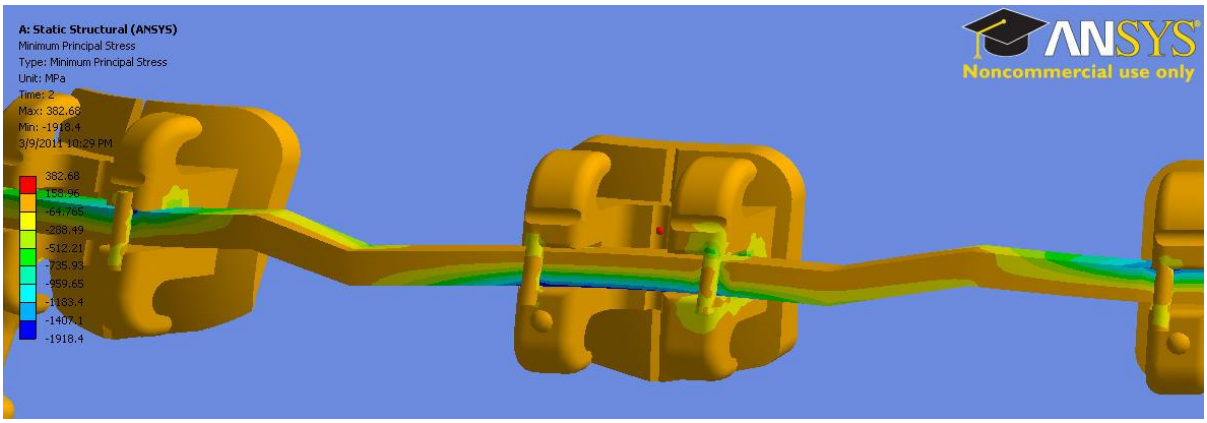

Figure 28. Tensile stress (minimum principal stress) distribution of the 0.019 x 0.025 inch stainless steel archwire activated with a 0.5 mm intrusive step into the lateral incisor bracket (middle).

Stress concentration can also be seen in the brackets (Figure 29) and as expected greater stress is present at the areas of contact between the wire and brackets. In a closer view (Figure 30) it can be appreciated that the wire causes higher stress at contact points at the far mesial and distal edges, but not as much in the center. All these model behaviors appeared consistent with physical behavior and clinical observations.

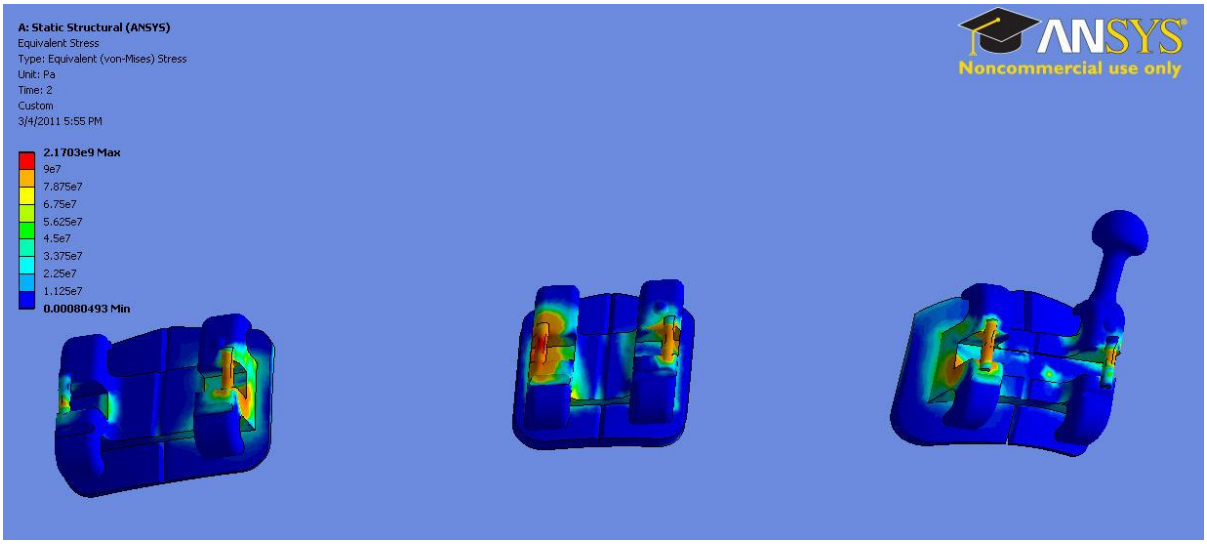

Figure 29. Equivalent (von-Mises) stress distribution of the anterior brackets after fully engaging the 0.019 x 0.025 inch stainless steel archwire with a 0.5 mm intrusive bend at the lateral incisor bracket (middle).

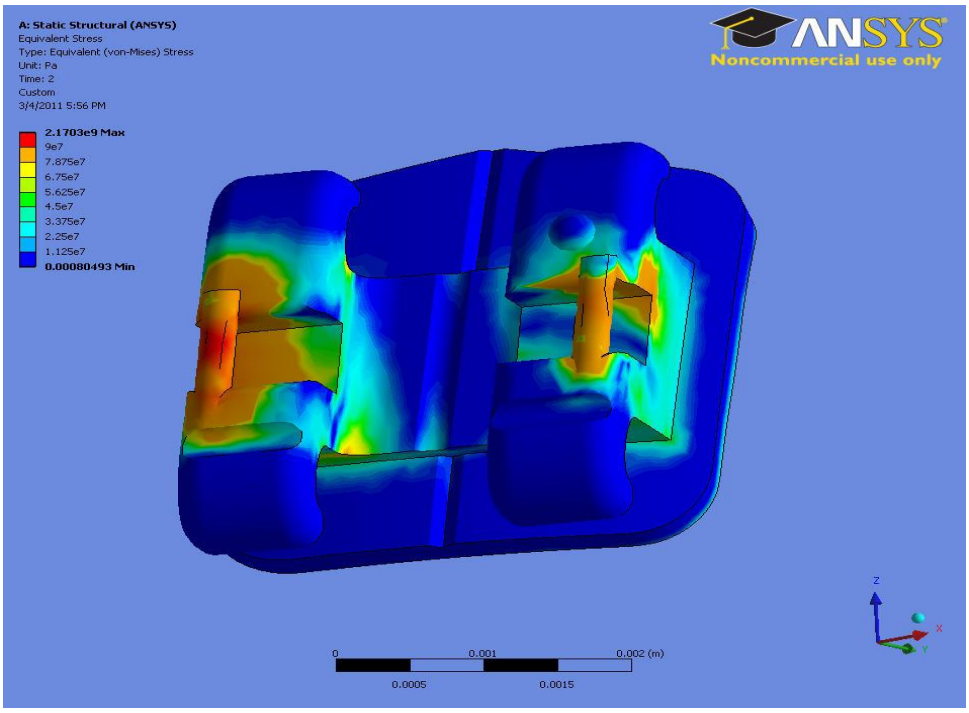

Figure 30. Equivalent (von-Mises) stress distribution of the lateral incisor bracket after fully engaging the archwire.

Aim 3. Labial and Lingual Comparison

Peak compressive stress was located at the lateral incisor archwire-bracket interface and values were 2170 MPa for the labial model and 3062 MPa for the lingual model. Table 5 shows much higher force was placed on the lingual bracket than at the labial bracket. Figures 31 and 32 show the force reaction at the contact between the wire and brackets. For the lateral incisor, the distance between the labial and lingual model centers of rotation was 0.00368 mm, and the shortest distance between labial and lingual bracket slots was 5.8 mm. The distance from the lateral incisor slot to the center of resistance for the labial system was 18.4 mm and for the lingual system was 16.5 mm. The difference in displacement of the lateral incisor crown was statistically significant ($p=0.04$, paired t test) when data of PDL model and steel model were pooled together. The locations of the anatomic points tracked to

make this comparison are shown in Figure 33. This suggested that there is a structure-associated difference in biomechanics, depending on where the brackets were placed. This difference was pronounced in the steel model (Figure 34) while diminished in the PDL model (Figure 35). The present result emphasizes the importance of incorporation of PDL in the study, which is not currently included in Badawi's testing machine (16).

Table 5. Bracket-Wire Reaction Force (N) for Labial and Lingual Models

	U1 Force	U2 Force	U3 Force
Labial	19.1	21.9	19.9
Lingual	18.4	37.2	15.4

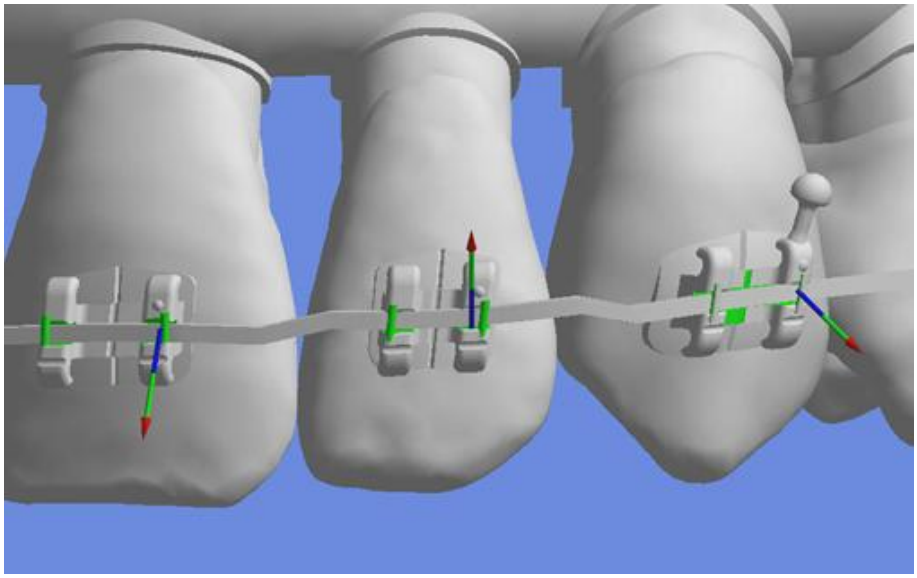

Figure 31. Reaction force directions for the labial system. Arrows indicate direction not magnitude.

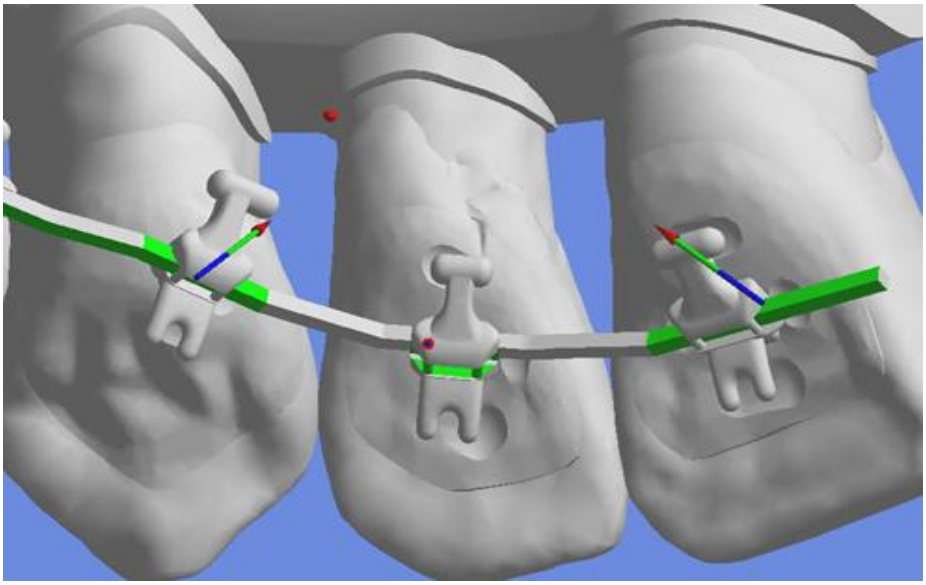

Figure 32. Reaction force directions for the lingual system. The direction for the lateral incisor is out of the page. Arrows indicate direction not magnitude.

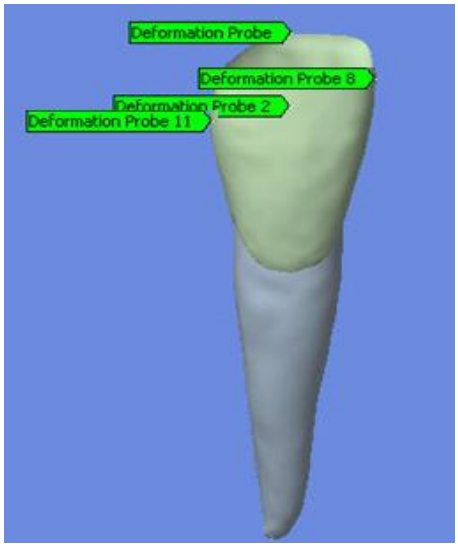

Figure 33. Location of anatomic points that were followed to track lateral incisor movement. Probe 1 is located at the incisal edge, probe 8 at the mesial contact point, probe 2 at the center of the incisal third of the crown, and probe 11 at the distal contact point.

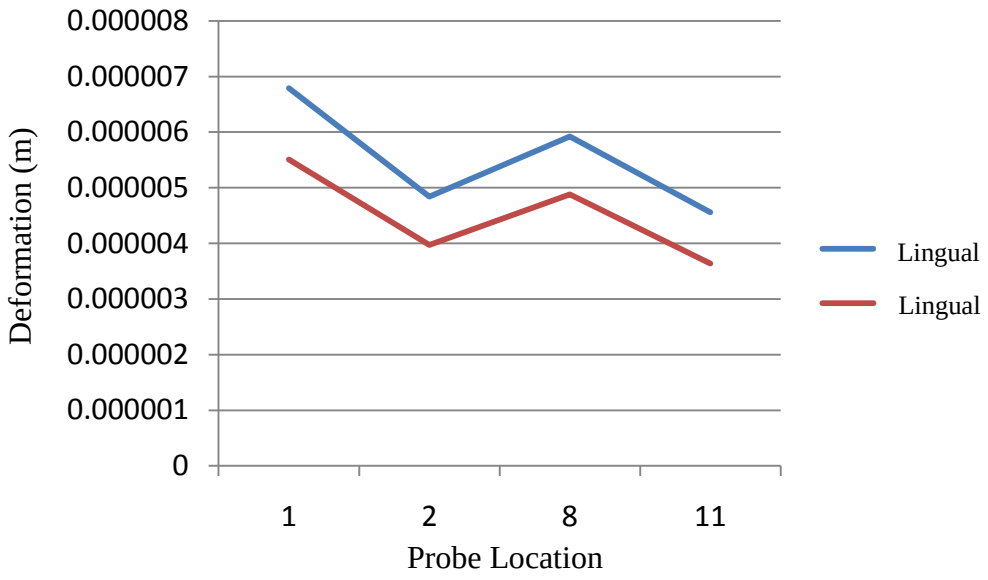

Figure 34. Deformation (mm) of steel model is shown at probe locations 1, 2, 8, and 11 for labial (red) and lingual (blue).

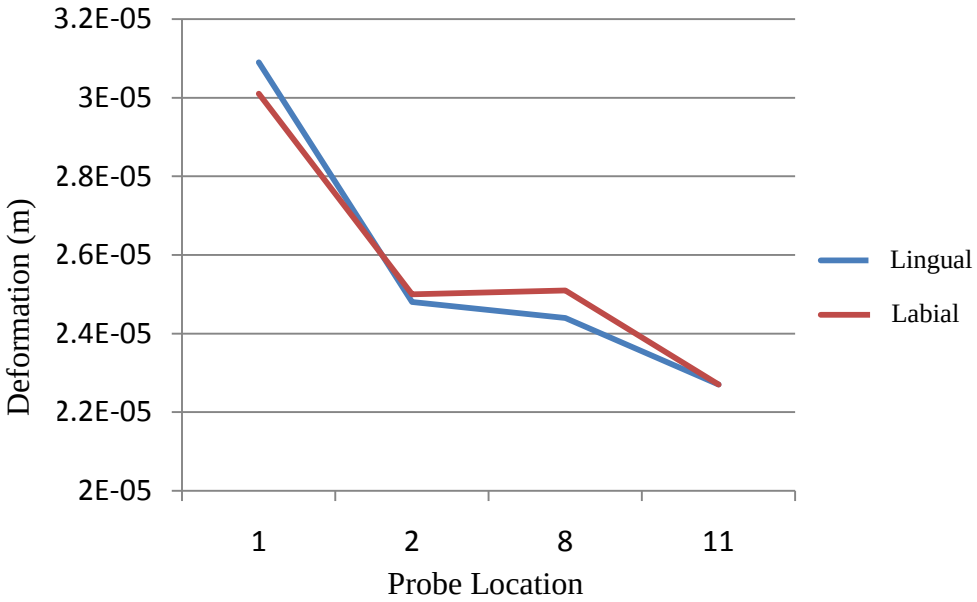

Figure 35. Deformation (mm) of PDL model is shown at probe locations 1, 2, 8, and 11 for labial (red) and lingual (blue).

Differences in the labial and lingual systems can be seen in Figures 36 and 37 where minimum principal elastic stress (compression) distribution is shown for the periodontal ligaments of all teeth. Visual analysis of the color map shows comparable stress distribution between the labial models. A higher level of stress was found at the facial alveolar crest of the lateral incisor with the lingual system (-8.93 MPa) than with the labial system (-7.12 MPa). Both systems show stress distribution consistent with facial tipping of the lateral incisor. Different centers of rotation can be seen in Figures 38 and 39.

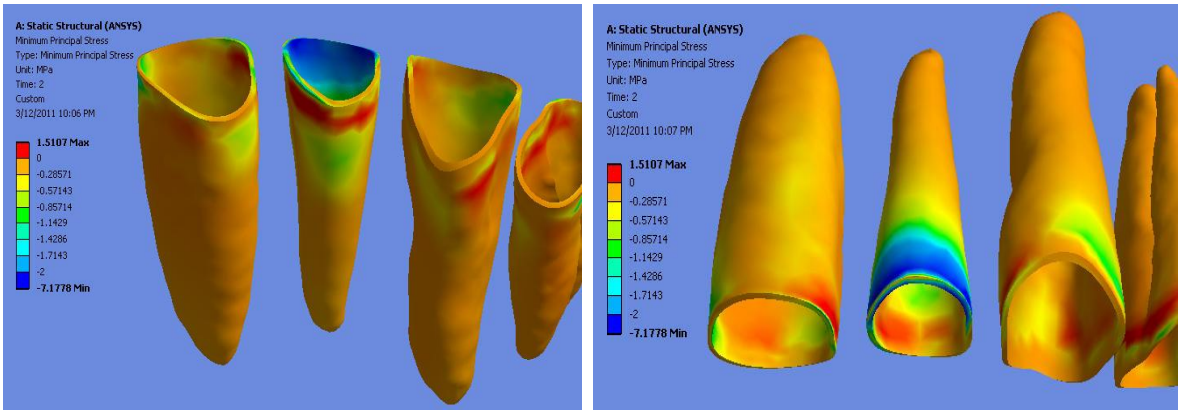

Figure 36. Labial system minimum principal elastic stress (compression) distribution. The color map shows highest compression blue.

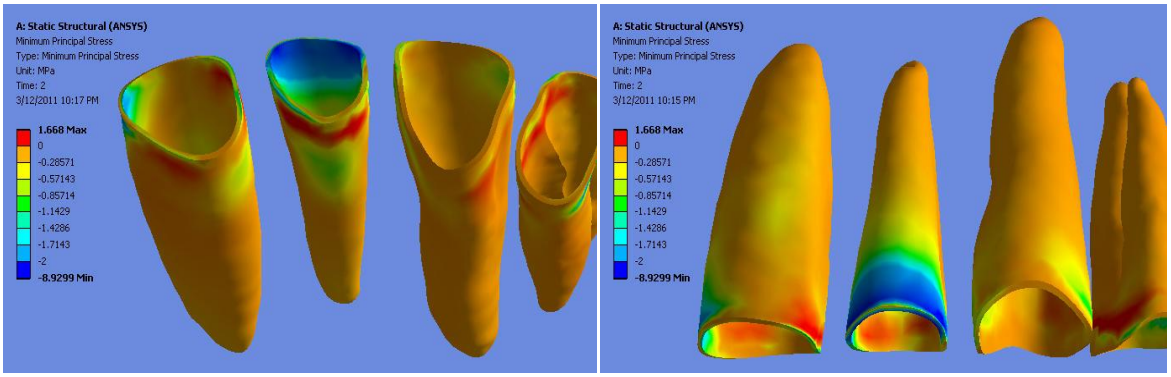

Figure 37. Lingual system minimum principal elastic stress (compression) distribution. The color map shows highest compression blue.

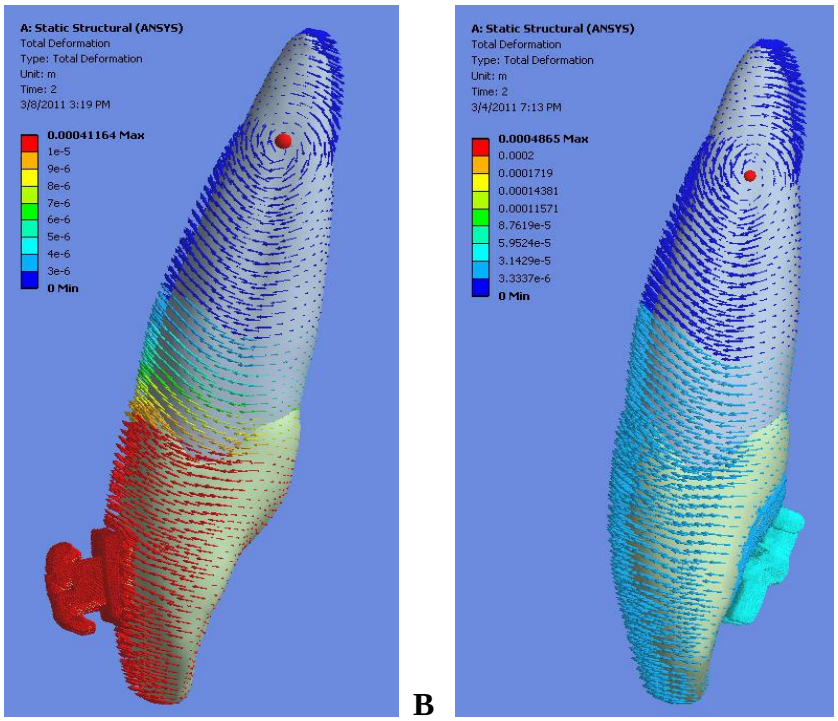

Figure 38. PDL model lateral incisor total deformation in the **A** labial system and **B** lingual system. Red dot is the center of rotation. Surrounding structures are transparent for display.

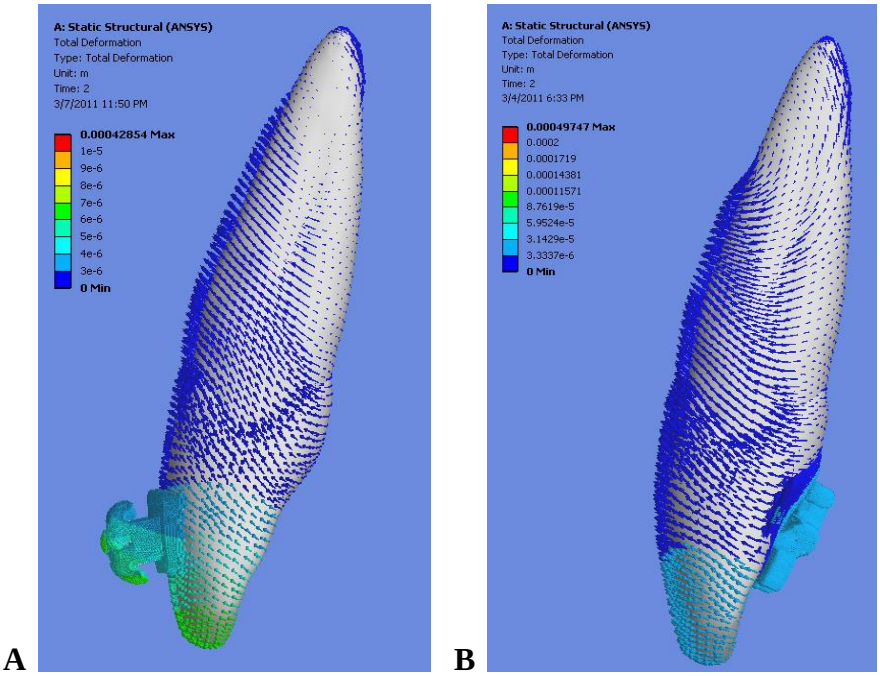

Figure 39. Steel model lateral incisor total deformation in the **A** labial system and **B** lingual system. Centers of rotation are between the canine and lateral incisor. Bone and surrounding structures are transparent for display.

V DISCUSSION

Aim 1. Advanced FE Model

Aim one consisted of first building a clinically advanced biomechanical model that approximates both the physical and the physiological behavior of human teeth and surrounding structures. Advancements in computational techniques in the finite element method have created useful models in industry, but there has not been much breakthrough in orthodontics. In the past, orthodontic FEA models consisted of limited approximations including rigid body structures, bonding teeth together, single tooth models, point forces on the teeth, one material throughout the entire model, and use of a simplified block of bone supporting the tooth. Recently, Cattaneo used accurate anatomy, two teeth and non-linear material properties and achieved a more realistic model with point forces applied (21). Merging the wire and the bracket system with proper anatomy seems to be a logical next step.

Our model not only used more realistic anatomy from the CT data but also used accurate structure for the wires and brackets from CAD design. Merging these complex systems created a model that provided answers to clinically relevant questions. More specifically using the labial system as an example, the reaction forces on the central incisor, the lateral incisor, and the canine were demonstrated to be outward and perpendicular to the facial surface. (Figure 31). The direction of these reaction forces appeared comparable to the forces measured in a multiple sensor station with a continuous wire reported by Badawi, indirectly validating our model (16).

As depicted in Figures 27 and 28, the deformation of the wire followed an expected pattern with compressive stress seen in areas contacting the bracket and tensile stress on the opposite side of the wire. Figure 26 shows the bending of the wire within the length of the bracket caused higher stress at the outer edges of the slot than in the middle. When considering the interaction between the wire and brackets as a simple beam element, the interaction is often considered a 3-node, pinned-pinned beam with a point force in the center. A more accurate representation would be 4-node, simple beam element with two equally concentrated loads symmetrically placed. The two point forces at the mid-span should represent the outer edges of the bracket slot. This phenomenon could only be revealed in the complete wire-bracket system, which has not been visualized before. This configuration of the archwire may have significant effects on notching of the archwire and merits further research.

Stress was also seen between the bracket and the wire at the premolar, which indicates an intrusive force at least two teeth away. Such remote effect is attributed to force propagation through a continuous wire.

Less than ideal ligation results in wires not being fully seated in the slot. This usually leads to incomplete expression of the wire in the first order for the labial brackets, and second order for the lingual brackets. The difference in order is due to the different path of insertion of the wire in both systems (6). Ligatures were placed against the archwire to eliminate any effects of loose ligation. When compared to the other parts of the bracket structure, they received a high level of stress indicating that they are an important addition to the model. Ligation of the wire into the bracket slot is often not considered in clinical orthodontics and warrants additional research.

Field et al (18) stated that contact points between teeth cause orthodontic forces to be transferred among teeth in a model. Neighboring dentition can cause greater compressive stresses since the PDL is affected by the rigidity of adjacent structures. Through the archwire and brackets, a force is applied on a tooth and reactive forces are generated in adjacent teeth. In both the PDL and steel models, stress was seen in the enamel contact points of adjacent teeth indicating transfer of orthodontic forces between the teeth. Stress in the bone extended far enough into the proximity of the adjacent teeth.

The reaction forces between the wire and brackets are shown in Table 1. Since the bracket wire system is the same in both models, differences should be attributed to the change of material property definitions. Different material properties generated different forces. Specifically, all force levels in the crowns, brackets and wires were higher for the stainless steel than for the PDL model. Rather than a compressible PDL damping the forces transferred to the bone, the stainless steel PDL clamped around the dentin essentially making the PDL part of the bone. Lighter forces in the PDL model can be explained by the elastic behavior of simulated human tissues as opposed to a stainless steel model.

Aim 2. Birth-Death Technique

In the clinic, a step bend is formed to provide intrusive force and hence intrusion to one or more teeth. Such an intrusive bend is placed in the bracket slot by forcing the stepped segment parallel to the slot opening and then inserting the wire into the bracket slot. After insertion the rebounding bend releases its stored elastic energy pushing the bracket-tooth complex toward the bone. To simulate the procedure of “engagement” and “rebound” force in the labial system, a 0.5mm intrusion bend was placed in the wire to demonstrate the use of the birth and death technique. Figures 22 through 24 illustrate the process of loading the

virtual archwire into the lateral incisor bracket. Stress levels increase in the adjacent brackets before the contact is activated in the lateral incisor bracket. Once the contact is activated and the displacement removed, the force is transferred from the adjacent brackets to the lateral incisor bracket. This essentially loads the wire into the bracket causing the force to be transferred from the adjacent teeth to the lateral incisor through the brackets and wire. The birth and death technique allows the anatomic model to merge with the bracket system model allowing analysis of stress resulting from different mechanical systems applied to the bracket/wire configuration.

Current FEA models rarely include brackets and even fewer have wires. When these are not present, a point force is often used in a manner that does not allow realistic expression of stress by the bracket system (15, 18, 26). Contact points between teeth are frequently rigidly fixed which can affect the results depending on the tooth movements being studied.

Similar studies have applied various combinations of point forces and moments, but none have applied an intrusive force with a bracket system. This makes a direct comparison to other research difficult. Cattaneo used combinations of forces levels and force-to-moment ratios to demonstrate that the position of the center of rotation varies (21). Figure 40 shows the stress distribution expected for uncontrolled tipping. When compared to the stress field for this model tipping can also be seen.

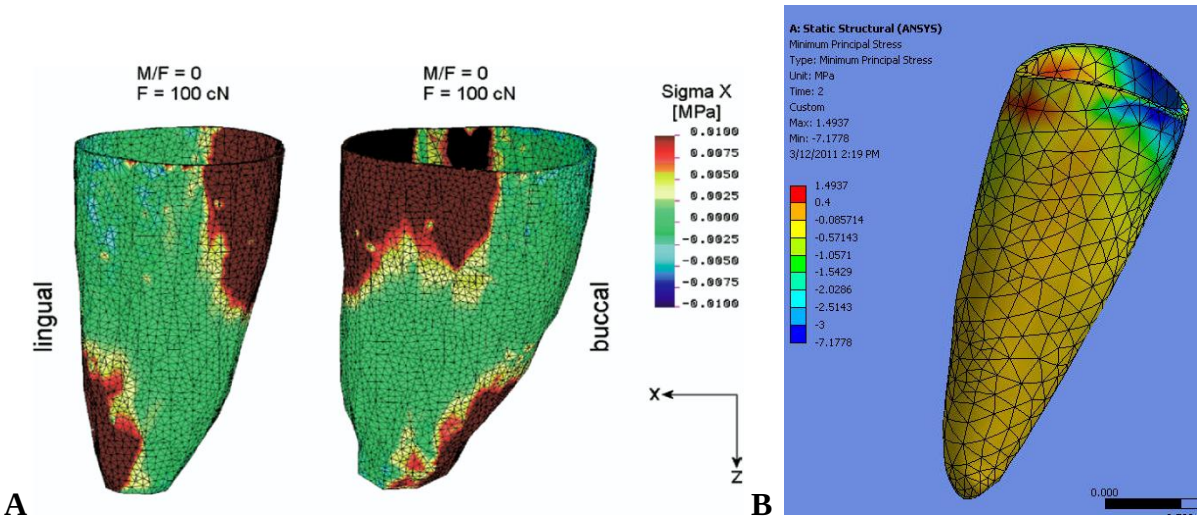

Figure 40. A. From Cattaneo (21), the stress field at premolar and canine when a 100cN horizontal point force is applied at the bracket shows uncontrolled tipping. **B.** Stress distribution with the 0.5mm intrusive bend in the labial bracket system.

Aim3. Intrusive Lingual Biomechanics

A 0.019 x 0.025 inch stainless steel archwire was selected as a common finishing wire for an 0.022-inch slot bracket system. In a clinical setting, a 0.5 mm intrusive step bend is a reasonable adjustment in the finishing stage of treatment. A 0.018 x 0.018 inch wire was selected given that is a common finishing wire size for the lingual system. Despite the fact that a TMA wire is more commonly used clinically, a stainless steel wire was used in the lingual appliance to allow direct comparison with the labial model. A 0.5 mm bend in a lingual appliance may be considered more pronounced than the same bend for the labial system (3, 5, 13). Considering the slot size alone, a 0.5 mm bend would have more effect in a 0.018 slot than a 0.022 slot. The lingual appliance should also have increased effect due to the shorter inter-bracket distances as opposed to labial systems

Moran (13) stated that shorter inter-bracket distance will cause an archwire to seem stiffer with the lingual system. Comparing conventional lingual brackets to labial brackets an

anterior inter-bracket distance ratio of 1:1.47 was found. With custom lingual brackets in our study the inter-bracket distance ratio was 1:1.21. This can be attributed to the narrower mesiodistal width of the custom lingual brackets over conventional lingual brackets. The relative stiffness of the wires is relative to these ratios and hence wires in our study would behave in a less stiff way than the ones reported by Moran.

Inter-bracket distance, play between the bracket and wire, and wire dimension are the key factors that determine the level of force applied by the bracket-wire system. Shorter inter-bracket distance and less play in the bracket would lead to the assumption that the lingual system will apply more force to the lateral incisor. However, an 0.018 x 0.018 inch archwire is less stiff than an 0.019 x 0.025 inch wire. As shown in Table 5, the net effect of these factors is that the labial appliance transferred less force (21.9 N) than the lingual (37.2 N).

When comparing the lateral incisor stress distribution in the PDL (Figures 37 and 38), similar compressive stress is seen at the facial surface near the alveolar crest with both systems. Due to the fact that lingual system point of force application is closer to the long axis of the tooth and the CR, a more homogeneous distribution of forces was expected. However, any advantage to prevent flaring that the lingual system might have had with bracket position was nullified by the higher level of force placed on the bracket. Both systems caused facial tipping of the lateral incisor.

In one of the few studies using the finite element analysis to examine the differences between labial and lingual force transfer, Liang et al (22) clearly demonstrated the force distribution through the PDL. A 3D FEM of a maxilla and maxillary incisors was constructed using ideal, generic morphology. An intrusive force (1.0 N), lingual retraction

force (0.64 N), and lingual root torque (-5 x10 -3 N-M) were applied. The same load was applied to nodes on the central and lateral incisors. The point force was selected at a location that would correspond to the center of a bracket on both labial and lingual sides. Results demonstrated that loads of the same magnitude can cause translation with the labial appliance and uncontrolled tipping with the lingual appliance. Liang concluded that lingual technique cannot simply follow the same clinical techniques used with labial appliances. When retracting incisors using lingual appliances, it would be necessary to increase lingual root torque and intrusive force. Lower horizontal retraction force may produce more controlled results.

Rather than applying forces and a moment at a specific point, our study used force applied through a bracket system. Relative to the lateral incisor, the applied force had intrusive and facial components as well as a moment of a couple from the rectangular wire interaction with the bracket slot. The intrusive bend should theoretically cause tipping. When considering the position of the bracket in relation to the center of rotation, more tipping was expected with the labial bracket system than with the lingual system(12). Figure 37 shows that the centers of rotation for both the labial and lingual systems, and the measured difference of 0.00368 mm not clinically significant. This also confirms that the applied force caused tipping.

Liang used an intrusive force (1.0 N), lingual retraction force (0.64 N), and lingual root torque (-5 x10 -3 N-M). The display of our results was modified to match those of Liang and a comparison of the total displacement is shown in Figure 41. As expected, both results demonstrate tipping with the lingual appliance around the center of rotation which is located within the dark blue region for each figure.

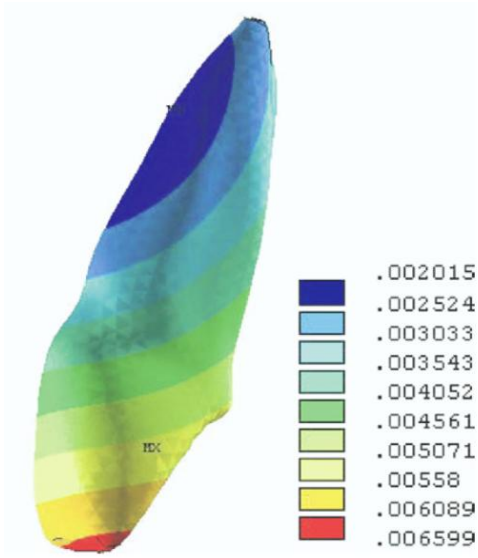

A

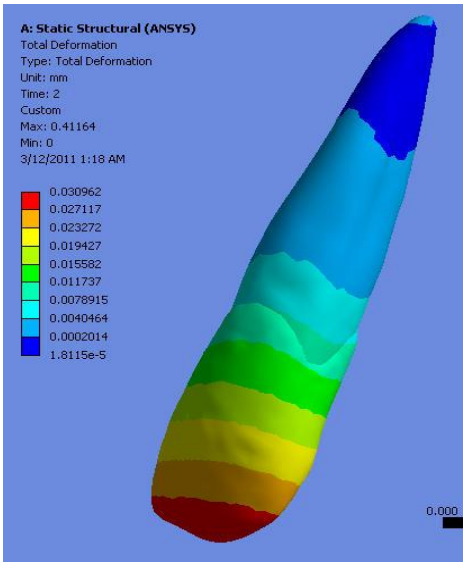

B

Figure 41. A. From Liang et al(22), Total Displacement of Maxillary Central Incisor with an 0.64-N intrusive force, 0.64-N retraction force, and a 5 x10 -3 N-M lingual root torque applied at a point on the lingual crown. **B.** Total displacement with the 0.5mm intrusive bend in the lingual bracket model.

VI CONCLUSIONS

The overall goal of this area of research is to develop a clinically advanced biomechanical model that approximates both the physical and the physiological behavior of human teeth and surrounding structures. Adding an accurate bracket-wire system is a step toward that goal. With the continuing development of computer capabilities and modeling techniques, these models could become a practical tool to assist in making clinical decisions.

1. Material property definitions have an effect on a finite element model.
2. The birth-death technique is a useful method to simulate the clinical effects of placing an archwire in brackets and allows forces to be transferred from the bracket-wire system to the surrounding dental structures.
3. The lingual appliance has different biomechanical effects than the labial appliance.

VII. REFERENCES

1. Russell JS. Aesthetic orthodontic brackets. J Orthod. 2005 Jun;32(2):146-63.

2. Noble J, Hechter FJ, Karaiskos NE, Lekic N, Wiltshire WA. Future practice plans of orthodontic residents in the United States. Am J Orthod Dentofacial Orthop. 2009 Mar;135(3):357-60.

3. Wiechmann D. A new bracket system for lingual orthodontic treatment. Part 2: First clinical experiences and further development. J Orofac Orthop. 2003 Sep;64(5):372-88.

4. Wiechmann D. Lingual orthodontics (part 1): laboratory procedure. J Orofac Orthop. 1999;60(5):371-9.

5. Wiechmann D. Lingual orthodontics (part 2): archwire fabrication. J Orofac Orthop. 1999;60(6):416-26.

6. Fuck LM, Wiechmann D, Drescher D. Comparison of the initial orthodontic force systems produced by a new lingual bracket system and a straight-wire appliance. J Orofac Orthop. 2005 Sep;66(5):363-76.

7. Fritz U, Diedrich P, Wiechmann D. Lingual technique--patients' characteristics, motivation and acceptance. Interpretation of a retrospective survey. J Orofac Orthop. 2002 May;63(3):227-33.

8. Hohoff A, Wiechmann D, Fillion D, Stamm T, Lippold C, Ehmer U. Evaluation of the parameters underlying the decision by adult patients to opt for lingual therapy: an international comparison. J Orofac Orthop. 2003 Mar;64(2):135-44.

9. Miyawaki S, Yasuhara M, Koh Y. Discomfort caused by bonded lingual orthodontic appliances in adult patients as examined by retrospective questionnaire. Am J Orthod Dentofacial Orthop. 1999 Jan;115(1):83-8.

10. van der Veen MH, Attin R, Schwestka-Polly R, Wiechmann D. Caries outcomes after orthodontic treatment with fixed appliances: do lingual brackets make a difference? Eur J Oral Sci. 2010 Jun;118(3):298-303.

11. Grauer D. Accuracy in tooth positioning with a fully customized lingual orthodontic appliance. Am J Orthod Dentofacial Orthop. (In Press).

12. Geron S, Romano R, Brosh T. Vertical forces in labial and lingual orthodontics applied on maxillary incisors--a theoretical approach. Angle Orthod. 2004 Apr;74(2):195-201.

13. Moran KI. Relative wire stiffness due to lingual versus labial interbracket distance. Am J Orthod Dentofacial Orthop. 1987 Jul;92(1):24-32.

14. Tanne K, Sakuda M, Burstone CJ. Three-dimensional finite element analysis for stress in the periodontal tissue by orthodontic forces. Am J Orthod Dentofacial Orthop. 1987 Dec;92(6):499-505.

15. Sung SJ, Jang GW, Chun YS, Moon YS. Effective en-masse retraction design with orthodontic mini-implant anchorage: a finite element analysis. Am J Orthod Dentofacial Orthop. 2010 May;137(5):648-57.

16. Badawi HM, Toogood RW, Carey JP, Heo G, Major PW. Three-dimensional orthodontic force measurements. Am J Orthod Dentofacial Orthop. 2009 Oct;136(4):518-28.

17. Cattaneo PM, Dalstra M, Melsen B. The finite element method: a tool to study orthodontic tooth movement. J Dent Res. 2005 May;84(5):428-33.

18. Field C, Ichim I, Swain MV, Chan E, Darendeliler MA, Li W, et al. Mechanical responses to orthodontic loading: a 3-dimensional finite element multi-tooth model. Am J Orthod Dentofacial Orthop. 2009 Feb;135(2):174-81.

19. Jones ML, Hickman J, Middleton J, Knox J, Volp C. A validated finite element method study of orthodontic tooth movement in the human subject. J Orthod. 2001 Mar;28(1):29-38.

20. Cattaneo PM, Dalstra M, Melsen B. Strains in periodontal ligament and alveolar bone associated with orthodontic tooth movement analyzed by finite element. Orthod Craniofac Res. 2009 May;12(2):120-8.

21. Cattaneo PM, Dalstra M, Melsen B. Moment-to-force ratio, center of rotation, and force level: a finite element study predicting their interdependency for simulated orthodontic loading regimens. Am J Orthod Dentofacial Orthop. 2008 May;133(5):681-9.

22. Liang W, Rong Q, Lin J, Xu B. Torque control of the maxillary incisors in lingual and labial orthodontics: a 3-dimensional finite element analysis. Am J Orthod Dentofacial Orthop. 2009 Mar;135(3):316-22.

23. Farah JW, Craig RG, Sikarskie DL. Photoelastic and finite element stress analysis of a restored axisymmetric first molar. J Biomech. 1973;60:511,511-20.

24. Tanne K, Yoshida S, Kawata T, Sasaki A, Knox J, Jones ML. An evaluation of the biomechanical response of the tooth and periodontium to orthodontic forces in adolescent and adult subjects. Br J Orthod. 1998 May;25(2):109-15.

25. Ammar HH, Ngan P, Crout RJ, Mucino VH, Mukdadi OM. Three-dimensional modeling and finite element analysis in treatment planning for orthodontic tooth movement. Am J Orthod Dentofacial Orthop. 2011 Jan;139(1):e59-71.

26. Kim T, Suh J, Kim N, Lee M. Optimum conditions for parallel translation of maxillary anterior teeth under retraction force determined with the finite element method. Am J Orthod Dentofacial Orthop. 2010 May;137(5):639-47.